International Journal for Parasitology: Drugs and Drug Resistance 6 (2016) 184–198

Contents lists available at ScienceDirect

International Journal for Parasitology: Drugs and Drug Resistance

journal homepage: www.elsevier.com/locate/ijpddr

# Exploring the scope of new arylamino alcohol derivatives: Synthesis, antimalarial evaluation, toxicological studies, and target exploration

Miguel Quiliano [a, b], Adela Mendoza [a], Kim Y. Fong [c], Adriana Pabón [d], Nathan E. Goldfarb [e, 1], Isabelle Fabing [f], Ariane Vettorazzi [g], Adela López de Cerain [g], Ben M. Dunn [e], Giovanny Garavito [h], David W. Wright [c], Eric Deharo [i], Silvia Pérez-Silanes [a, b], Ignacio Aldana [a, b], Silvia Galiano [a, b, *]

[a] Department of Organic and Pharmaceutical Chemistry, Faculty of Pharmacy and Nutrition, University of Navarra, Pamplona, 31008, Spain
[b] Institute of Tropical Health (ISTUN), University of Navarra, Pamplona, 31008, Spain
[c] Department of Chemistry, Vanderbilt University, Station B 351822, Nashville, TN 37235, USA
[d] Grupo Malaria, Universidad de Antioquía, Medellín, Colombia
[e] Department of Biochemistry and Molecular Biology, University of Florida, Gainesville, FL, USA
[f] Laboratoire de Synthèse et Physicochimie de Molécules d'Intérêt Biologique SPCMIB – UMR5068, CNRS - Université Paul Sabatier, 118, route de Narbonne, 31062, Toulouse Cedex 09, France
[g] Department of Pharmacology and Toxicology, Faculty of Pharmacy and Nutrition, University of Navarra, Pamplona, 31008, Spain
[h] Universidad Nacional de Colombia, Sede Bogotá, Facultad de Ciencias, Departamento de Farmacia (DFUNC), Grupo de investigación FaMeTra (Farmacología de la Medicina tradicional y popular), Carrera 30 45-03, Bogotá D.C., Colombia
[i] UMR 152 PHARMA-DEV, Université Toulouse, IRD, UPS, 31062, Toulouse, France

ARTICLE INFO

*Article history:*
Received 23 May 2016
Accepted 26 September 2016
Available online 28 September 2016

*Keywords:*
Antimalarial
Antiplasmodial
Arylamino alcohol
Plasmepsin II enzyme
Hemozoin inhibition
Mannich reaction

ABSTRACT

Synthesis of new 1-aryl-3-substituted propanol derivatives followed by structure-activity relationship, *in silico* drug-likeness, cytotoxicity, genotoxicity, *in silico* metabolism, *in silico* pharmacophore modeling, and *in vivo* studies led to the identification of compounds **22** and **23** with significant *in vitro* antiplasmodial activity against drug sensitive (D6 $IC_{50} \leq 0.19$ μM) and multidrug resistant (FCR-3 $IC_{50} \leq 0.40$ μM and C235 $IC_{50} \leq 0.28$ μM) strains of *Plasmodium falciparum*. Adequate selectivity index and absence of genotoxicity was also observed. Notably, compound **22** displays excellent parasitemia reduction (98 ± 1%), and complete cure with all treated mice surviving through the entire period with no signs of toxicity. One important factor is the agreement between *in vitro* potency and *in vivo* studies. Target exploration was performed; this chemotype series exhibits an alternative antimalarial mechanism.



## 1. Introduction

Malaria, a major tropical disease for which no long-term sustainable treatment is available, continues to affect large parts of the world. According to the latest World Malaria Report, 3.2 billion people in 96 countries are at risk of being infected. In 2015 alone, 214 million cases were reported globally resulting in an estimated 438,000 deaths mainly consisting of African children and pregnant women (WHO, 2015). This life-threatening disease is caused by *Plasmodium* species with *Plasmodium falciparum* (*P. falciparum*) being the most deadly. Currently, first-line therapy includes artemisinin-based combination therapies (ACT) (Delves et al., 2012; Wells et al., 2015); however, in recent years parasite resistance against artemisinin and its derivatives has emerged and spread along the Cambodia-Thailand border (Ashley et al., 2014; Tun et al., 2015). To address this challenge, new antimalarial entities are needed. Although recent efforts in antimalarial drug discovery have focused on new targets, nonclassical chemical scaffolds, and vaccines (Biamonte et al., 2013; Barnett and Guy, 2014; Wells et al., 2015), extensive studies on classical antimalarial chemotypes or drug repurposing are needed due to the high cost and time required

* Corresponding author. Departament of Organic and Pharmaceutical Chemistry, Faculty of Pharmacy and Nutrition, Institute of Tropical Health (ISTUN), University of Navarra, Irunlarrea 1, Pamplona, 31008, Navarra, Spain.
*E-mail address:* sgaliano@unav.es (S. Galiano).
[1] Present address: Department of Pharmaceutical and Biomedical Sciences, College of Pharmacy, California Health Sciences University, Clovis, CA, USA.

http://dx.doi.org/10.1016/j.ijpddr.2016.09.004

in the drug discovery and development process (Andrews et al., 2014; Biamonte, 2014).

One classic antimalarial chemotype present in potent antimalarial drugs, including quinine (1), mefloquine (2), lumefantrine (3), and halofantrine (4), is the arylamino alcohol (ß-amino or γ-amino alcohol moiety). The structural requirements for antiplasmodial activity include the presence of an aromatic and amino alcohol portion linked by a carbon chain of two or three atoms in length (Bhattacharjee and Karle, 1996) (Fig. 1). Based on this antiplasmodial pharmacophore, antimalarial amino alcohols continue to attract the interest of various research groups due to their high biological activity and ADMET values. Representative studies of the ß-amino alcohol moiety include the works of Guy et al. who performed the optimization of propafenone analogues (Lowes et al., 2011, 2012) as a product of high throughput screening (Weisman et al., 2006), and Smith and Chibale et al. who developed totarol (Clarkson et al., 2003; Tacon et al., 2012) and chalcone (Hans et al., 2010), respectively, as natural product-like hybrid derivatives. In addition, mefloquine and 4-aminoquinoline derivatives are valid synthetic approaches explored by Milner et al. (2010) and Kobarfard et al. (2012), respectively, among other studies (Robin et al., 2007; D'hooghe et al., 2011). However, there are only a few examples of the γ-amino alcohol moiety reported in the last thirteen years (D'hooghe et al., 2009; Perez-Silanes et al., 2009; Mendoza et al., 2011; Quiliano and Aldana, 2013). D'hooghe et al. (2009) reported a wide range of antiplasmodial activity against the chloroquine sensitive *P. falciparum* strain D10; however, submicromolar values were not reached (6 μM ≤ $IC_{50}$ ≤ 175 μM). Thus, further studies on the unexplored γ-moiety as a source of new antimalarial drugs are needed.

Our research on γ-amino alcohols explored the structure-activity relationship (SAR) of 1-aryl-3-susbtituted propanol derivatives (APD) with promising results (Perez-Silanes et al., 2009; Mendoza et al., 2011; Quiliano and Aldana, 2013). Initial SAR studies showed that all of the aryl-ketone derivatives were inactive against 3D7, NF54, and FCR-3 strains of *P. falciparum* (Perez-Silanes et al., 2009; Mendoza et al., 2011). In contrast, APD were active against 3D7 (0.19 ≤ $IC_{50}$ ≤ 0.38 μM) (Perez-Silanes et al., 2009), NF54 (1.3 ≤ $IC_{50}$ ≤ 8 μM) (Mendoza et al., 2011), and FCR-3 (0.5 ≤ $IC_{50}$ ≤ 10 μM) (Mendoza et al., 2011) strains of *P. falciparum*. However, low parasitemia reduction (≤65%) was observed in the *in vivo Plasmodium berghei* (*P. berghei*) mouse model. Interestingly, linker reduction in one carbon atom between the alcohol and amine portion (γ-to ß-amino alcohol) in APD reduced the activity by half. Previous, *in silico* studies proposed plasmepsin II (PM2) as a putative target for APD (Mendoza et al., 2011), but has yet to be confirmed experimentally. Nonetheless, more studies with APD are necessary to be validated as potential antimalarial hits (MMV, 2008).

Thus, exploration and development of APD as antimalarials requires (1) expanding SAR studies, (2) generating additional analogues with high potency against both chloroquine sensitive and multidrug resistant strains of *P. falciparum*, (3) improving parasitemia reduction in the *P. berghei* mouse model, (4) establishing a safe toxicological profile, and (5) exploring biological targets in *P. falciparum*.

In this study, we expanded the chemical scope in the antimalarial framework by preparing new APD for testing their antiplasmodial activity *in vitro* against *P. falciparum* (sensitive and resistant strains) and *in vivo* against *P. berghei*. Chiral separation and enantiomeric testing were also conducted. Further, cytotoxicity and genotoxicity studies were performed on active compounds and potential metabolites. Since target validation is a crucial step in the drug discovery process, APD compounds were evaluated for their ability to inhibit both the PM2 enzyme and the hemozoin formation pathway. Finally, pharmacophore modeling studies were performed on APD.

## 2. Material and methods

### 2.1. Synthesis of APD compounds

The methods used for synthesizing the final compounds (**14**–**26**) are presented in Schemes 1 and 2. The synthetic method has been published previously (Perez-Silanes et al., 2009; Mendoza et al., 2011). The starting arylamines 2-nitro-4-trifluoromethyl phenyl piperazine, 4-(4-fluorophenyl)-1,2,3,6-tetrahydropyridine and 4-trifluoromethyl phenyl piperazine were commercially

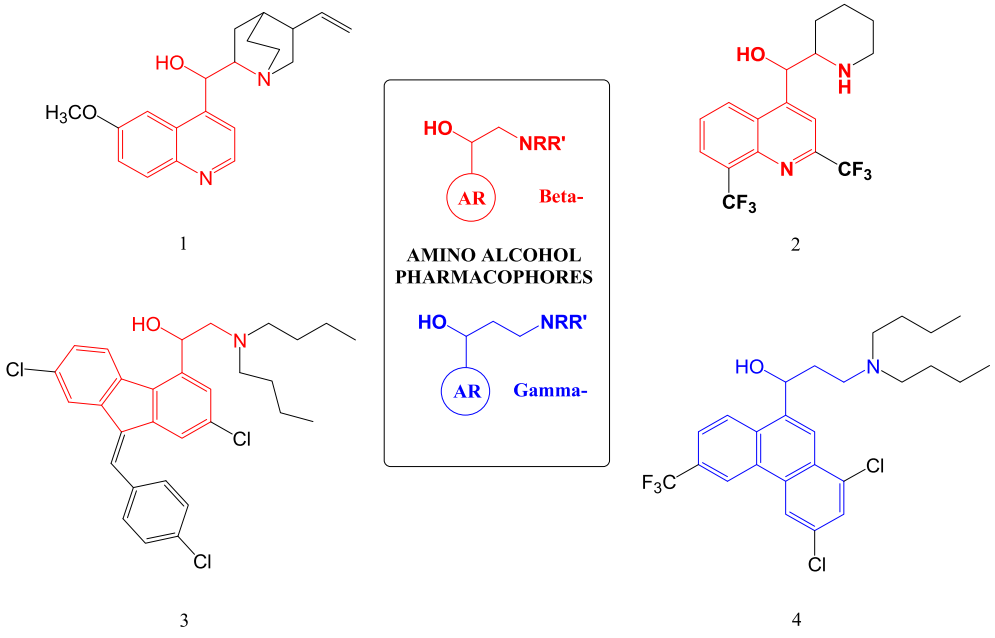


**Fig. 1.** Antimalarial drugs with amino alcohol moiety as a pharmacophore: (1) quinine; (2) mefloquine; (3) lumefantrine; (4) halofantrine.

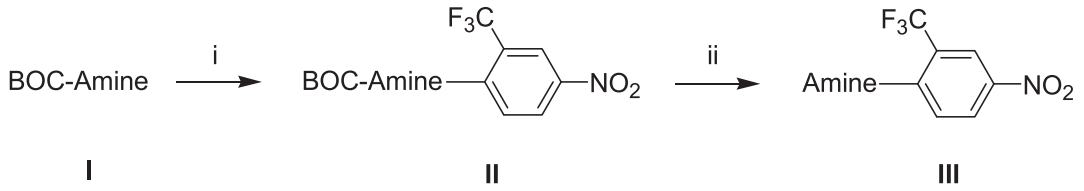


*Reagents and conditions:* (i) 2-fluoro-5-nitrobenzotrifluoride, acetonitrile, $K_2CO_3$, 12 hours; (ii) acetic acid/ hydrochloric acid (1:1), rt., 2 hours, NaOH (2M)

**Scheme 1.** Synthesis of arylamines not commercially available.

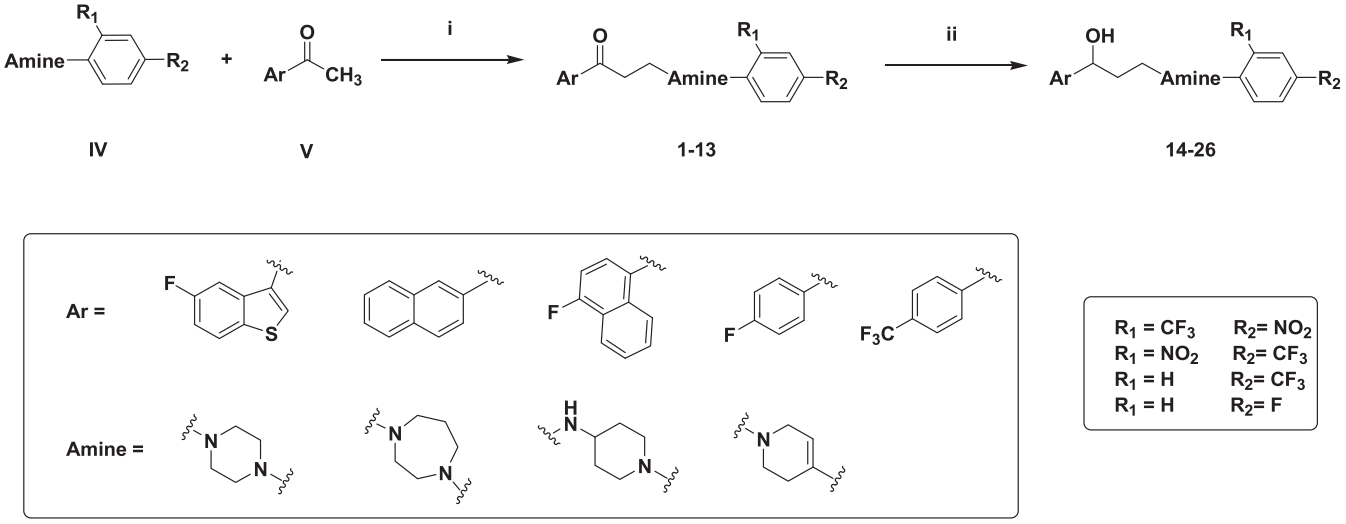


*Reagents and conditions*: (i) 1,3-dioxolane, hydrochloric acid, 130-140ºC, NaOH 2M; (ii) methanol, sodium borohydride, 0ºC, 2 hours.

**Scheme 2.** Synthesis of arylamino alcohols **14**–**26.**

available. Non-commercially available arylamines were synthesized using the corresponding BOC-amine (**I**) and 2-fluoro-4-nitrobenzotrifluoride by an Ar-$S_N$' reaction via Meisenheimer complex formation and subsequent removal of the BOC-group with HCl and acetic acid (Scheme 1). All methyl ketone precursors (**V**) were commercially available. The ketone intermediates (β-amino ketones) (**1**–**13**) were prepared by condensation of the corresponding methyl ketone (**V**) with the different aryl amines (**IV**) via Mannich reaction (Scheme 2). The hydroxyl derivatives (γ-amino alcohols) (**14**–**26**) were obtained by reduction of the corresponding carbonyl group with $NaBH_4$ in methanol (Scheme 2).

### 2.2. Experimental section

#### 2.2.1. Reagents and instruments

Chemical reagents and solvents were purchased from commercial companies and were used without further purification. All of the synthesized final compounds were chemically characterized by thin layer chromatography (TLC), melting point (mp) and proton and carbon nuclear magnetic resonance ($^1$H NMR and $^{13}$C NMR) spectra as well as by elemental microanalysis. Purity was determined by high performance liquid chromatography (HPLC). Final compounds were confirmed to have ≥96% purity. $^1$H NMR and $^{13}$C NMR spectra were recorded on a Bruker 400 Ultrashield (Rheinstetten, Germany) operating at 400 and 100 MHz, respectively, using tetramethylsilane (TMS) as the internal standard and chloroform ($CDCl_3$) or dimethyl sulfoxide-$d_6$ (DMSO-$d_6$) as solvents. The chemical shifts are reported in ppm ($\delta$) and the coupling constant ($J$) values are given in Hertz (Hz). Elemental microanalyses were obtained on an Elemental Analyzer (LECO CHN-900, Michigan, USA) from vacuum-dried samples. The analytical results for C, H, and N were within ±0.4 of the theoretical values. Alugram SIL G/UV254 (Layer: 0.2 mm) (Macherey-Nagel, Germany) was used for TLC and silica gel 60 (0.040–0.063 mm and 0.063–0.200 nm) was used for column chromatography (Merck). Some final derivatives were purified by automated flash chromatography with a binary gradient of dichloromethane (DCM) (synthesis grade SDS-Carlo Erba Reactifs, France) and methanol (MeOH) (Panreac Química S.A.) and UV variable dual-wavelength detection. The chromatography was developed using the CombiFlash® Rf (Teledyne Isco, Lincoln. USA) with DCM/MeOH as solvents and a normal phase of 12 g Flash Column (RediSep® Rf Columns by Teledyne Isco, Inc., USA). HPLC experiments were developed on an Ultimate 3000 Chromatograph (Dionex) with Chromeleon v.6.8 software. The measurements were performed using an RP 18 column (Lichrospher 100 RP 18 E.C. 5 μm; 10 × 0.46 cm; Teknokroma) as the

stationary phase at a flow rate of 1 mL/min and with MeOH/water (80:20) as the mobile phase. The retention times ($t_R$) are expressed in minutes and the reference wavelength is set at 254 nm. Compounds **II** and **III** were synthesized as previously described (Perez-Silanes et al., 2009; Mendoza et al., 2011).

*2.2.2. General synthetic methods*

*2.2.2.1. General method 1 for the synthesis of ketone derivatives (**1**–**13**).* The corresponding substituted aryl methyl ketone (**V**) (1.0 equiv) and the aryl amine (**IV**) (1.0 equiv) was dissolved in 1,3-dioxolane (1.4%) and concentrated HCl (1 mL) was added until pH 1–2 was reached. The resulting mixture was heated at reflux for 1–2 h. NaOH (2 M) was then added (50 mL) and the product was extracted with DCM (3 × 50 mL). The organic phase was dried with anhydrous $Na_2SO_4$, filtered, and evaporated to dryness under reduced pressure. The residue was purified by column chromatography on silica gel using DCM/MeOH 95:5 (v/v) as eluent or automated flash chromatography eluting with DCM/MeOH 99:1 (v/v). In other cases, the hydrochloride salt was prepared by adding a hydrogen chloride ethereal solution to the stirred compounds. Spectral data for selected ketone derivatives is shown at Supplementary Data section.

*2.2.2.2. General method 2 for the synthesis of hydroxyl derivatives (**14**–**26**).* Sodium borohydride (3.0 equiv) was added dropwise to a pre-cooled suspension (0 °C) of the corresponding ketone (**V**) (1.0 equiv) in MeOH over a period of 30–60 min. The solvent was removed under reduced pressure and the residue was dissolved in DCM (40 mL) and then washed with water (3 × 30 mL). The organic phase was dried with anhydrous $Na_2SO_4$ and filtered. After evaporating the solvent to dryness under reduced pressure, the compound was purified by column chromatography (SP: silica gel) eluting with DCM/MeOH 99:1 (v/v) or automated flash chromatography eluting with DCM/MeOH 99:1 (v/v). Selected compounds were converted to hydrochloride salts by adding a hydrogen chloride ethereal solution to the stirred compounds.

*2.2.2.3. 1-(5-fluorobenzo[b]thiophen-3-yl)-3-[4-(4-nitro-2-trifluoromethylphenyl)piperazin-1-yl] propan-1-ol (**14**).* Yield: 21%, mp 140-142 °C. $^1$H NMR (DMSO-$d_6$, 400 MHz) $\delta$ ppm: 8.46, 8.49 (dd, 1H, $J$ = 9.0 Hz, $J$ = 2.5 Hz); 8.42 (d, 1H, $J$ = 2.6 Hz); 8.04 (q, 1H, $J$ = 8.8 Hz, $J$ = 5.1 Hz); 7.82,7.83 (dd, 1H, $J$ = 10.3 Hz, $J$ = 2.4 Hz); 7.77 (s, 1H); 7.65 (d, 1H, $J$ = 9.0 Hz); 7.27 (dt, 1H, $J$ = 8.9 Hz, $J$ = 2.4 Hz); 5.82 (br s, 1H); 5.05 (br s, 1H); 3.64 (d, 2H); 3.42–3.50 (m, 6H); 3.17 (br s, 2H); 2.23,2.30 (dd, 2H) ppm. $^{13}$C NMR (DMSO-$d_6$, 100 MHz) $\delta$: 162.07; 159.65; 156.10; 151.77; 143.58; 140.66 (d, $J$ = 4.6 Hz); 139.18 (d, $J$ = 8.4 Hz); 136.75; 129.60; 126.26; 125.43 (d, $J$ = 9.0 Hz); 125.13; 124.56 (d, $J$ = 6.8 Hz); 113.78 (d, $J$ = 25.4 Hz); 109.15 (d, $J$ = 23.6 Hz); 66.45; 54.19; 51.92 (2C); 50.05 (2C); 31.81 ppm. Anal. Calcd for $C_{22}H_{21}N_3F_4O_3S$: C, 54.65%; H, 4.38%; N, 8.64%; Found: C, 54.83%; H, 4.44%; N, 8.99%.

*2.2.2.4. Hydrochloride of 1-(5-fluorobenzo[b]thiophen-3-yl)-3-[4-(2-nitro-4-trifluoromethyl phenyl)piperazin-1-yl] propan-1-ol (**15**).* Yield: 20%, mp 196-198 °C. $^1$H NMR (400 MHz, DMSO-$d_6$) $\delta$: 8.20 (s, 1H), 8.02 (dd, 1H, $J$ = 8.9 Hz, 5.1 Hz), 7.90 (d, 1H, $J$ = 8.4 Hz), 7.77 (d, 1H, $J$ = 10.2 Hz), 7.72 (s, 1H), 7.49 (d, 1H, $J$ = 8.5 Hz), 7.26 (dt, 1H, $J$ = 9.1 Hz, 8.8 Hz, 2.2 Hz), 5.00 (br s, 1H), 3.70 (br s, 2H), 3.24 (br s, 4H), 2.92 (bs, 4H), 2.06 (br s, 2H) ppm. $^{13}$C NMR (DMSO-$d_6$, 100 MHz) $\delta$: 161.98; 159.61; 147.87; 140.78; 139.33 (d, $J$ = 9.0 Hz); 136.73; 131.20 (d, $J$ = 3.1 Hz); 126.02; 125.68; 125.41 (d, $J$ = 9.1 Hz); 124.60 (q, $J$ = 4.1 Hz); 122.98; 122.74; 113.71 (d, $J$ = 25.4 Hz); 109.06 (d, $J$ = 23.2 Hz); 74.12; 66.99; 54.88 (2C); 52.35 (2C); 48.23 ppm. Anal. Calcd for $C_{22}H_{21}N_3F_4O_3S$.HCl: C, 50.81%; H, 4.23%; N, 8.08%; Found: C, 51.20%; H, 3.85%; N, 8.11%.

*2.2.2.5. 1-(5-fluorobenzo[b]thiophen-3-yl)-3-(4-(4-trifluoromethylphenyl)piperazin-1-yl) propan-1-ol (**16**).* Yield: 15%, mp 158-160 °C. $^1$H NMR (400 MHz, $CDCl_3$) $\delta$: 7.80 (br s, 1H), 7.50–7.54 (m, 4H), 7.10–7.15 (m, 1H), 6.96 (d, 2H, $J$ = 8.4 Hz), 5.32 (dd, 1H, $J$ = 4.1 Hz, 6.7 Hz), 3.45 (br s, 4H), 2.93–2.94 (m, 3H), 2.82 (br s, 3H), 2.21 (bs, 2H) ppm. $^{13}$C NMR ($CDCl_3$, 100 MHz) $\delta$: 162.20; 159.80; 153.44; 139.83 (d, $J$ = 4.4 Hz); 138.71 (d, $J$ = 9.1 Hz); 136.76 (d, $J$ = 1.4 Hz); 126.88 (2C, q, $J$ = 3.8 Hz); 126.44; 124.64; 124.41(d, $J$ = 9.4 Hz); 115.19 (2C); 113.51 (d, $J$ = 25.2 Hz); 108.29 (d, $J$ = 23.4 Hz); 71.97; 57.57; 53.40 (2C); 48.51 (2C); 31.87 ppm. Anal. Calcd for $C_{22}H_{22}N_2F_4OS$: C, 60.26%; H, 5.06%; N, 6.39%; Found: C, 60.30%; H, 4.95%; N, 6.24%.

*2.2.2.6. 1-(5-fluorobenzo[b]thiophen-3-yl)-3-[4-(4-nitro-2-trifluoromethylphenyl)-1,4-diazepan-1-yl]propan-1-ol (**17**).* Yield: 25%, mp 110-111 °C. $^1$H NMR (400 MHz, $CDCl_3$) $\delta$: 8.54 (s, 1H), 8.28 (dd, 1H, $J$ = 9.2 Hz, 2.7 Hz), 7.80 (dd, 1H, $J$ = 8.8 Hz, 5.0 Hz), 7.51 (dd, 1H, $J$ = 9.8 Hz, 1.5 Hz), 7.50 (s, 1H), 7.22 (d, 1H, $J$ = 9.2 Hz), 7.12 (dd, 1H, $J$ = 8.8 Hz, 2.4 Hz), 5.62 (br s, 2H), 5.30 (t, 1H, $J$ = 5.7 Hz), 3.54 (br s, 2H), 2.98–2.99 (m, 2H), 2.87–2.93 (m, 4H), 2.08 (br s, 4H) ppm. $^{13}$C NMR ($CDCl_3$, 100 MHz) $\delta$: 162.18; 159.78; 157.28; 151.76; 140.69; 139.90 (d, $J$ = 4.7 Hz); 138.68 (d, $J$ = 8.9 Hz); 136.76 (d, $J$ = 1.3 Hz); 127.92; 125.78 (q, $J$ = 5.9 Hz); 124.62; 124.40 (d, $J$ = 9.4 Hz); 121.74; 113.49 (d, $J$ = 25.0 Hz); 108.26 (d, $J$ = 23.4 Hz); 72.07; 57.69; 56.35; 55.68; 55.37; 54.64; 32.60; 28.04 ppm. Anal. Calcd for $C_{23}H_{23}N_3F_4O_3S$: C, 55.53%; H, 4.66%; N, 8.45%; Found: C, 55.15%; H, 4.64%; N, 8.26%.

*2.2.2.7. 1-(5-fluorobenzo[b]thiophen-3-yl)-3-[1-(4-nitro-2-trifluoromethylphenyl)piperidin-4-yl]amino)propan-1-ol (**18**).* Yield: 37%, mp 140-142 °C. $^1$H NMR (400 MHz, $CDCl_3$) $\delta$: 8.53 (br s, 1H), 8.33 (dd, 1H, $J$ = 8.5 Hz, 1.8 Hz), 7.79 (dd. 1H, $J$ = 8.2 Hz, 3.1 Hz), 7.52 (s, 1H), 7.50 (dd, 1H, $J$ = 8.5 Hz, 4.9 Hz), 7.29 (d, 1H, $J$ = 8.6 Hz), 7.12 (t, 1H, $J$ = 7.7 Hz), 5.30 (d, 1H, $J$ = 7.7 Hz), 3.42 (d, 2H, $J$ = 9.0 Hz), 3.13 (br s, 2H), 2.95 (t, 2H, $J$ = 9.7 Hz), 2.75 (br s, 1H), 2.11 (br s, 3H), 1.95–1.97 (m, 1H), 1.56–1.71 (m, 2H) ppm. $^{13}$C NMR ($CDCl_3$, 100 MHz) $\delta$: 162.16; 159.76; 157.67 (d, $J$ = 1.4 Hz); 151.76; 142.37; 140.10 (d, $J$ = 4.4 Hz); 138.67 (d, $J$ = 9.5 Hz); 136.78 (d, $J$ = 1.2 Hz); 128.18; 125.11 (q, $J$ = 5.7 Hz); 124.65; 124.38 (d, $J$ = 9.4 Hz); 122.71; 113.43 (d, $J$ = 25.0 Hz); 108.25 (d, $J$ = 23.4 Hz); 72.13; 54.52; 52.34 (2C); 45.72; 35.80; 32.94 (2C) ppm. Anal. Calcd for $C_{23}H_{23}N_3F_4O_3S$: C, 55.53%; H, 4.66%; N, 8.45%; Found: C, 55.55%; H, 4.62%; N, 8.44%.

*2.2.2.8. 3-[4-(4-fluorophenyl)-3,6-dihydropyridin-1(2H)-yl]-1-(naphthalen-2-yl)propan-1-ol (**19**).* Yield:23%, mp 127-129 °C. $^1$H NMR (400 MHz, $CDCl_3$) $\delta$: 7.91 (s, 1H), 7.87 (dd, 1H, $J$ = 7.8 Hz, 2.3 Hz), 7.85 (d, 2H, $J$ = 8.3 Hz), 7.51 (dd, 1H, $J$ = 7.4 Hz, 1.6 Hz), 7.45–7.50 (m, 2H), 7.37 (dd, 2H, $J$ = 8.7 Hz, 5.4 Hz), 7.04 (t, 2H, $J$ = 8.7 Hz), 6.02 (s, 1H), 5.17 (br s, 1H), 3.31 (d, 2H, $J$ = 16.7 Hz), 2.72–2.96 (m, 4H), 2.64 (s, 2H), 1.99–2.12 (m, 2H) ppm. $^{13}$C NMR ($CDCl_3$, 100 MHz) $\delta$: 163.81; 161.35; 142.52; 136.88 (d, $J$ = 2.9 Hz); 134.67; 133.82; 133.13; 128.36 (d, $J$ = 4.4 Hz); 128.06; 126.86 (2C, d, $J$ = 7.9 Hz); 126.40; 125.95; 124.48 (2C, d, $J$ = 12.8 Hz); 121.08; 115.60 (2C, d, $J$ = 21.3 Hz); 75.80; 56.89; 53.55; 50.42; 34.29; 28.27 ppm. Anal. Calcd for $C_{24}H_{24}NFO.½H_2O$: C, 77.74%; H, 6.74%; N, 3.77%; Found: C, 77.87%; H, 6.82%; N, 3.40%.

*2.2.2.9. 3-[4-(4-fluorophenyl)-3,6-dihydropyridin-1(2H)-y])-1-(4-(trifluoromethylphenyl)propan-1-ol (**20**).* Yield: 40%, mp 116-117 °C. $^1$H NMR (400 MHz, DMSO-$d_6$) $\delta$: 7.68 (d, 2H, $J$ = 8.1 Hz), 7.57 (d, 2H, $J$ = 7.9 Hz), 7.47 (dd, 2H, $J$ = 8.4 Hz, 5.6 Hz), 7.15 (t, 2H, $J$ = 8.8 Hz), 6.12 (s, 1H), 5.70 (br s, 1H), 4.75–4.80 (m, 1H), 3.08 (s, 2H), 2.62 (t, 2H, $J$ = 5.5 Hz), 2.45–2.50 (m, 4H), 1.81 (dd, 2H, $J$ = 13.7 Hz, 7.3 Hz) ppm. $^{13}$C NMR (DMSO-$d_6$, 100 MHz) $\delta$: 160.98; 151.87; 137.40 (d, $J$ = 3.0 Hz); 133.82; 128.30; 127.99; 127.30 (2C); 127.22; 126.64;

125.73 (2C, d, $J = 4.0$ Hz); 122.82; 115.89 (2C, d, $J = 21.2$ Hz); 71.49; 55.32; 53.60; 50.74; 36.96; 28.36 ppm. Anal. Calcd for $C_{21}H_{21}NF_4O$: C, 66.49%; H, 5.54%; N, 3.69%; Found: C, 66.11%; H, 5.67%; N, 3.81%.

*2.2.2.10. Hydrochloride of 1-(4-fluoronaphthalen-1-yl)-3-(4-(4-(trifluoromethylphenyl) piperazin-1-yl) propan-1-ol (**21**).* Yield; 45%, mp 174-175 °C. $^1$H NMR (400 MHz, DMSO-$d_6$) $\delta$: 11.12 (br s, 1H), 8.29 (d, 1H, $J = 8.8$ Hz), 8.10 (d, 1H, $J = 6.6$ Hz), 7.67 (br s, 3H), 7.56 (d, 2H, $J = 8.4$ Hz), 7.36 (dd, 1H, $J = 8.2$ Hz, 9.7 Hz), 7.13 (d, 2H, $J = 8.1$ Hz), 5.90 (br s, 1H), 5.41 (d, 1H, $J = 7.5$ Hz), 3.97 (br s, 2H), 3.20–3.30 (m, 6H), 3.55 (br s, 2H), 2.21 (d, 2H) ppm. $^{13}$C NMR (DMSO-$d_6$, 100 MHz) $\delta$: 159.34; 152.87; 137.93; 129.53; 127.72; 127.21 (2C); 126.81; 125.01; 124.62; 124.34; 123.92 (d, $J = 9.1$ Hz); 123.67; 121.37 (d, $J = 6.0$ Hz); 115.76 (2C); 109.94; 67.62; 54.46; 51.64 (2C); 45.23 (2C); 32.94 ppm. Anal. Calcd for $C_{24}H_{24}N_2F_4O$.HCl: C, 61.47%; H, 5.39%; N, 5.98%; Found: C, 61.35%; H, 5.02%; N, 5.96%.

*2.2.2.11. 1-(4-Fluoronaphthalen-1-yl)-3-((1-(4-nitro-2-(trifluoromethyl)phenyl)piperidin-4-yl) amino) propan-1-ol (**22**).* Yield: 90%, mp 93-95 °C. $^1$H NMR (400 MHz $CDCl_3$) $\delta$: 8.53 (d, 1H, $J = 2.7$ Hz), 8.33 (dd, 1H, $J = 9.0$ Hz, 2.7 Hz), 8.16 (dd, 1H, $J = 7.2$ Hz, 3.3 Hz), 8.04 (d, 1H, $J = 7.8$ Hz), 7.67–7.72 (m, 1H), 7.53–7.61 (m, 2H), 7.27–7.30 (m, 1H), 7.17 (dd, 1H, $J = 10.2$ Hz, 8.1 Hz), 5.71 (dd, 1H, $J = 8.2$ Hz, 2.3 Hz), 3.42 (d, 2H), 3.08–3.15 (m, 1H), 3.00–3.03 (m, 1H), 2.98 (t, 2H, $J = 11.5$ Hz), 2.75–2.84 (m, 1H), 2.12 (d, 1H, $J = 12.7$ Hz), 2.15–2.23 (m, 2H), 1.86–2.01 (m, 1H), 1.68–1.83 (m, 2H) ppm. $^{13}$C NMR ($CDCl_3$, 100 MHz) $\delta$: 159.75; 157.66; 157.26; 142.39; 136.42 (d, $J = 3.7$ Hz); 131.74 (d, $J = 4.2$ Hz); 128.18; 127.16; 126.06; 125.12 (d, $J = 5.4$ Hz); 124.66; 124.22; 123.33 (d, $J = 2.8$ Hz); 123.24 (d, $J = 8.5$ Hz); 122.72; 121.76 (d, $J = 5.8$ Hz); 109.25 (d, $J = 19.5$ Hz); 72.58; 54.56; 52.32 (2C); 45.74; 36.95; 32.88 (2C) ppm. Anal. Calcd for $C_{25}H_{25}N_3F_4O_3$: C, 61.10%; H, 5.09%; N, 8.55%; Found: C, 60.77%; H, 5.43%; N, 8.30%.

*2.2.2.12. 1-(4-Fluoronaphthalen-1-yl)-3-[4-(4-fluorophenyl)-3,6-dihydropyridin-1(2H)-yl] propan-1-ol (**23**).* Yield: 82%, mp 162-163 °C. $^1$H NMR (400 MHz. DMSO-$d_6$) $\delta$: 8.20 (dd, 1H, $J = 7.0$ Hz, 2.5 Hz), 8.07 (d, 1H, $J = 8.2$ Hz), 7.70 (dd, 1H, $J = 8.0$ Hz, 5.6 Hz), 7.54–7.61 (m, 2H), 7.35–7.40 (m, 2H), 7.18 (dd, 1H, $J = 10.2$ Hz, 8.1 Hz), 7.00–7.08 (m, 2H), 6.00–6.05 (m, 1H), 5.74 (br s, 1H), 3.47 (d, 1H, $J = 11.3$ Hz), 3.41 (d, 1H, $J = 11.2$ Hz), 2.84–3.12 (m, 4H), 2.73 (br s, 2H), 2.14–2.20 (m, 2H) ppm. $^{13}$C NMR (DMSO-$d_6$, 100 MHz) $\delta$: 160.99; 159.06; 139.11 (d, $J = 4.2$ Hz); 137.42 (d, $J = 3.2$ Hz); 133.87; 131.99 (d, $J = 4.3$ Hz); 127.79; 127.31 (2C, d, $J = 8.0$ Hz); 127.02 (d, $J = 1.6$ Hz); 124.55 (d, $J = 2.6$ Hz); 123.77 (d, $J = 1.0$ Hz); 123.65 (d, $J = 8.8$ Hz); 122.91 (d, $J = 1.4$ Hz); 121.30 (d, $J = 5.8$ Hz); 115.92 (2C, d, $J = 21.2$ Hz); 109.82 (d, $J = 19.2$ Hz); 68.80; 55.72; 53.85; 50.82; 36.75; 28.43 ppm. Anal. Calcd for $C_{24}H_{23}NF_2O$: C, 75.99%; H, 6.07%; N, 3.69%; Found: C, 75.65%; H, 6.45%; N, 3.50%.

*2.2.2.13. Hydrochloride of 1-(4-fluorophenyl)-3-[4-(4-nitro-2-trifluoromethylphenyl) piperazin-1-yl]propan-1-ol (**24**).* Yield: 20%, mp 163-165 °C, $^1$H NMR (400 MHz, DMSO-$d_6$) $\delta$: 11.20 (br s, 1H), 8.47 (d, 1H, $J = 8.8$ Hz), 8.42 (s, 1H), 7.64 (d, 1H, $J = 9.0$ Hz), 7.42 (dd, 2H, $J = 8.0$ Hz, 6.6 Hz), 7.18 (t, 2H, $J = 8.1$ Hz), 5.65 (s, 1H), 4.69 (s, 1H), 3.60 (br s, 2H), 3.35–3.44 (m, 4H), 3.15–3.20 (m, 4H), 2.09 (bs, 2H) ppm. $^{13}$C NMR (DMSO-$d_6$, 100 MHz) $\delta$: 162.08; 159.50; 154.72; 150.40; 142.21; 140.75 (d, $J = 2.3$ Hz); 128.22 (2C); 127.09 (d, $J = 8.1$ Hz); 123.74; 123.21 (d, $J = 5.2$ Hz); 114.35 (2C, d, $J = 21.0$ Hz); 66.47; 54.20; 52.04 (2C); 50.07 (2C); 31.83 ppm. Anal. Calcd for $C_{20}H_{21}N_3F_4O_3$ .HCl.$H_2O$: C, 49.85%; H, 5.02%; N, 8.72%; Found: C, 49.50%; H, 4.76%; N, 8.63%.

*2.2.2.14. Hydrochloride of 1-(4-fluorophenyl)-3-[1-(4-nitro-2-trifluoromethylphenyl) piperidin-4-yl)amino]propan-1-ol (**25**).* Yield: 11%, mp 185-187 °C, $^1$H NMR (400 MHz, DMSO-$d_6$) $\delta$: 8.37 (br s, 2H), 7.50 (d, 1H, $J = 8.0$ Hz), 7.36 (br s, 2H), 7.13 (t, 2H, $J = 8.1$ Hz), 5.61 (s, 1H); 4.69 (t, 1H, $J = 9.0$ Hz), 3.20–3.30 (m, 2H), 2.95 (t, 2H, $J = 12.1$ Hz), 2.63–2.64 (m, 2H), 2.58 (br s, 1H), 1.90 (d, 2H, $J = 11.0$ Hz), 1.70 (br s, 2H), 1.38 (br s, 2H) ppm. $^{13}$C NMR (DMSO-$d_6$, 100 MHz) $\delta$: 163.06; 160.66; 157.70; 143.19 (d, $J = 2.7$ Hz); 141.73; 129.21; 128.34 (2C, d, $J = 8.0$ Hz); 124.98 (q, $J = 6.0$ Hz); 123.88; 122.82; 115.49 (2C, d, $J = 21.1$ Hz); 71.59; 54.24; 52.08 (2C); 44.00; 35.62; 32.34 (2C) ppm. Anal. Calcd for $C_{21}H_{23}N_3F_4O_3$ .HCl: C, 52.51%; H, 5.03%; N, 8.80%; Found: C, 52.13%; H, 4.91%; N, 8.49%.

*2.2.2.15. 1-(4-fluorophenyl)-3-[4-(4-fluorophenyl)-3,6-dihydropyridin-1(2H)-yl]propan-1-ol (**26**).* Yield: 12%, mp 199-201 °C. $^1$H NMR (400 MHz, DMSO-$d_6$) $\delta$: 7.46 (dd, 2H, $J = 7.7$ Hz, 5.5 Hz), 7.37 (dd, 2H, $J = 7.9$ Hz, 6.0 Hz), 7.14 (dd, 4H, $J = 12.6$ Hz, 8.0 Hz), 6.12 (br s, 1H), 5.49 (br s, 1H), 4.66 (t, 1H, $J$=6.3 Hz), 3.06 (br s, 2H), 2.57–2.62 (m, 2H), 2.45 (br s, 4H), 1.76–1.80 (m, 2H) ppm. $^{13}$C NMR (DMSO-$d_6$, 100 MHz) $\delta$: 160.98; 159.80; 141.53; 139.87 (d, $J = 3.0$ Hz); 133.85; 128.40 (2C, d, $J = 8.0$ Hz); 127.78; 127.25 (2C, d, $J = 8.0$ Hz); 115.80 (2C, d, $J = 21.2$ Hz); 115.29 (2C, d, $J = 21.0$ Hz); 71.89; 55.87; 53.57; 50.62; 36.96; 28.34 ppm. Anal. Calcd for $C_{20}H_{21}NF_2O.¼H_2O$: C, 71.88%; H, 6.43%; N, 4.19%; Found: C, 72.06%; H, 6.33%; N, 4.03%.

### 2.3. Separation and testing of the APD enantiomers

The separation of enantiomers involved two steps: analytical scale chiral chromatography and preparative scale chiral chromatography. For analytical chromatography, an isocratic method was developed on the ACQUITY UltraPerformance Convergence Chromatography System™ (UPC$^2$)® from Waters. The fast screening strategy was performed testing organic modifiers (MeOH, isopropanol (*i*-Pr), and diethylamine (DEA), all HPLC grade in the $CO_2$ mobile phase and 5 chiral columns (Chiralpak IA, OD, AD, OJ and IC, 100 × 4.6 mm i.d. column, Chiral Technologies, Daicel Group). The mobile phase composition was controlled by four pumps. The pump head used for the carbon dioxide was cooled. The mobile phase conditions were optimized to obtain efficient elution times and separation factors. The analytical flow rate was 3.5 mL/min. The outlet pressure was 130 bar and the columns were maintained at 40 °C. The PDA detector was set at 342 nm. Injection volume was 10 μL. The best conditions were obtained using Chiralpak IC column with 20% of *i*-Pr + 0.1% DEA as an additive in the $CO_2$ mobile phase. The retention times for each of the enantiomers were $rt_1 = 4.65$ min and $rt_2 = 5.60$ min.

For the enantiomeric separation of compound **25**, supercritical preparative scale chromatography was performed on a Purification Prep 80 system (Waters). Chiral separation was run on Chiralpak IC column, 5 μm (20 × 250) mm column (Chiral Technologies, Daicel Group) eluted with a mixture of $CO_2$ and 15% of *i*-Pr + 0.1% DEA. The working flow was 80 mL/min. The automated back pressure valve was regulated to 130 bar and the oven temperature was 40 °C. The UV detection was performed at 342 nm. The injection volume was 1 mL of an upstream filtered concentrated solution of 5 g/L of *i*-Pr in stacked mode. All fractions containing enantiomers 1 and 2 were collected in the same bottles A and B, respectively. Finally, each enantiomer and racemic mixture of compound **25** were evaluated against *P. falciparum* F32 Tanzania strain (chloroquine sensitive) according to Bouquet et al. (2012).

### 2.4. In vitro antiplasmodial activity (FCR-3 strain)

The multidrug resistant FCR-3 strain of *P. falciparum* was cultured at 37 °C in a pure gas mixture of 5% $O_2$, 5% $CO_2$, and 90% $N_2$ environment in RPMI 1640 medium supplemented with 25 mM

HEPES, 5% (w/v) $NaHCO_3$, 0.1 mg/mL gentamicin, and 10% $A^+$ heat-inactivated human serum, as previously described (Trager and Jensen, 1976). Compounds were dissolved in DMSO and tested with final concentrations ranging between 0.1 and 200 μM. The final DMSO concentration was never greater than 0.1%. *In vitro* antimalarial activity was measured using the [$^3$H]-hypoxanthine (MP Biomedicals, USA) incorporation assay (Desjardins et al., 1979) with some modifications. All experiments were performed in triplicate. Results were expressed as the concentration resulting in 50% inhibition ($IC_{50}$) which was calculated by linear interpolation (Huber and Koella, 1993) as follow:

$$\mathrm{Log}(IC_{50}) = \mathrm{Log}(X1) + \frac{(50 - Y1)}{(Y2 - Y1)}[\mathrm{Log}(X2) - \mathrm{Log}(X1)]$$

Where:

X1: concentration of the drug that gives a % inhibition of the parasitemia Y1>50%
X2: concentration of the drug that gives a % inhibition of the parasitemia Y2<50%
% Inhibition of the incorporation of labeled hypoxanthine = 100-(P/T*100)
P: counts per minute for every concentration
T: negative control (red blood cells without drug)

### 2.5. In vivo antimalarial activity

Studies were conducted according to the French and Colombian guidelines on laboratory animal use and care (N° 2001-464 and N° 008430, respectively). The classical 4-day suppressive test was carried out as follows (Peters, 1970). Swiss male mice weighing 20 ± 2 g, were infected with $10^7$ *P. berghei* ANKA parasitized cells (day 0). Two hours after infection and at the same time during 4 consecutive days, batches of three to five mice were orally treated at a dose of 50 mg/kg/day (drugs were dissolved in vehicle, water:DMSO). A control group received the vehicle while a reference group was orally administered chloroquine diphosphate at 3 mg/kg/day. Survival of the mice was checked daily and the percentage of parasitized erythrocytes was determined on day 4 by Giemsa-stained thin blood smears made from peripheral blood.

### 2.6. Cytotoxicity assay

VERO cells (African Green Monkey kidney epithelial cells) were seeded ($5 \times 10^5$ cells/mL, 100μL/well) in a 96-well flat-bottom plate at 37 °C and with 5% $CO_2$ in phenol red free RPMI 1640 (Sigma) supplemented with 10% heat-inactivated fetal bovine serum. Compounds were added at varying concentrations and the cells were cultured for 48 h. The effect was determined using the 3-(4,5-dimethylthiazol-2-yl)-2,5-diphenyltetrazolium bromide (MTT) viability assay (Mosmann, 1983). Four hours after the addition of MTT, 100 μL of lysis buffer (50% *i*-Pr, 30% water, 20% (w/v) SDS) was added and the cells were incubated at room temperature for 15 min under agitation. Finally, optical density was read at 590 nm with a 96-well scanner (Bio-Rad). All experiments were performed in triplicate. The $GI_{50}$ determined by linear regression analysis was defined as the concentration of test sample resulting in 50% inhibition of cell proliferation compared to controls.

### 2.7. In silico physicochemical properties calculation

Virtual Computational Chemistry Laboratory (Tetko et al., 2005) (http://www.vcclab.org/) and Molinspiration online property calculation toolkit (http://www.molinspiration.com/cgi-bin/properties) were used to calculate Topological Polar Surface Area (TPSA) (Ertl et al., 2000), ALOGPs2.1, number of rotatable bonds and violations of Lipinski's rule of five (Lipinski et al., 1997). In addition, human intestinal absorption (%ABS) was calculated using the following approach of Zhao et al. (2002):

$$\%ABS = 109 - (0.345 \times TPSA)$$

### 2.8. Genotoxicity assay

The SOS/*umu* test was used to determine the DNA-damaging effect and was carried out according to the method of Oda et al. (1985) and Reifferscheid et al. (1991) with some modifications. The test strain *Salmonella typhimurium* TA1535/pSK1002 (German Collection for microorganisms and cell cultures (DSMZ) was thawed from stock (−80 °C; in TGA medium containing 10% DMSO as cryoprotective agent) and 0.5 mL of bacteria was resuspended in 100 mL TGA medium supplemented with ampicillin (50 μg/mL). The test strain suspension was incubated overnight at 37 °C with slight orbital shaking (155 rpm) until an optical density was reached ($OD_{600}$ between 0.5 and 1.5). Then, the overnight culture was diluted with fresh TGA medium (not supplemented with ampicillin) and incubated for 2 h at 37 °C, 155 rpm, in order to obtain a log-phase bacterial growth culture ($OD_{600}$ between 0.15 and 0.4). The test was performed in the absence and presence of an external metabolic activation system (10% of rat S9 mix, prepared from S9 SD rat liver Aroclor KCl frozen, Trinova, Germany), in order to also determine the possible genotoxic effects of any metabolite. In each test performed negative and positive controls were included with DMSO used as the negative control and 4-nitroquinoline-*N*-oxide (4-NQO) (Sigma-Aldrich, China) and 2-aminoanthracene (2-AA) (Sigma-Aldrich, Germany) used as positive controls in the absence and presence of S9 mix, respectively.

Test procedure was as follows: first, each compound tested was dissolved in DMSO at 40 mg/mL (for a final assay concentration of 1 mg/mL) and 11 serial ½ dilutions were prepared in a 96-well plate (plate A; final volume in each well was 10 μL). In case where cell survival was <80% in the lowest concentration tested, new 11 serial ½ dilutions at lower concentrations were prepared. The highest concentrations of DMSO used for the positive controls were 100 μg/mL for 4-NQO (final concentration: 2.5 μg/mL) and 0.5 mg/mL for 2-AA (final concentration: 0.0125 mg/mL). Then, 70 μL of water was added to each well and evaluated in order to detect any precipitation of the compounds. In two other 96-well plates (plates B; one with S9 and the other without S9), 10 μL S9 mix or 10 μL PBS, respectively were added and afterwards, 25 μL of each concentration of compound previously prepared. Finally, 90 μL of exponentially growing bacteria was added to each well and both plates were incubated for 4 h by shaking (500 rpm) at 37 °C. After the incubation period, the $OD_{600}$ was measured in order to evaluate toxicity on *S. typhimurium* TA1535/pSK1002.

Toxicity was calculated as follows:

$$\text{Survival percentage} = \left(\frac{A_{600nm} \text{ for each concentration tested}}{\text{Media } A_{600nm} \text{ for negative control}}\right) \times 100\%$$

Afterwards, for the determination of β-galactosidase activity, in two new 96-well plates (plates C) 150 μL ONPG solution (2-nitrophenyl-β-D-galactopyranoside, Sigma-Aldrich, Switzerland) (0.9 mg/mL in B-buffer prepared according to Reifferscheid et al. (1991) was added to each well and 30 μL of the content of each

well of the plates B was transferred to plates C. Both plates were incubated 30 min by shaking (500 rpm) at 28 °C avoiding direct light exposure. After the incubation period, the reaction was stopped by adding 120 μL of $Na_2CO_3$ (1M). Absorbance at 420 nm was then measured immediately, and β-galactosidase activity (relative units; RU) was calculated as follows:

$$\beta\ \text{galactosidase enzymatic units} = \frac{A_{420nm}\ \text{for each concentration tested}}{A_{600nm}\ \text{for each concentration tested}}$$

And finally, the induction factor (IF) was calculated as follows:

$$IF = \frac{\beta\ \text{galactosidase RU for each concentration tested}}{\text{Average}\ \beta\ \text{galactosidase RU for negative control}}$$

Where:

$$\text{Average}\ \beta\ \text{galactosidase RU for negative control} = \frac{\text{Average}\ A_{420nm}\ \text{for negative control}}{\text{Average}\ A_{600nm}\ \text{for negative control}}$$

In the same way, β-galactosidase relative units were calculated for both positive controls and the test was only considered valid if the positive controls reached an induction factor ≥2 under the given test conditions.

Thus, a compound was considered genotoxic when in any of the conditions studied (with or without metabolic activation) the IF of the *umu* operon was ≥2 at non-cytotoxic concentrations (bacteria survival percentage ≥80%). Any well where compound precipitation was observed was discarded from analysis.

### 2.9. In vitro antiplasmodial activity (D6 and C235 strains)

A chloroquine sensitive (D6, obtained from Walter Reed Army Institute of Research) and multidrug resistant (C235, obtained from Walter Reed Army Institute of Research) strain of *P. falciparum* were continuously cultured following modifications to the original Trager and Jensen method (1976). Each strain was maintained at 5% hematocrit using human $A^+$ erythrocytes and incubated at 37 °C in a pure gas mixture of 5% $O_2$, 5% $CO_2$, and 90% $N_2$. Culture media included RPMI 1640 with L-glutamine and supplemented with 25 mM HEPES, 11 mM glucose, 29 μM hypoxanthine, 29 mM sodium bicarbonate, and 10% human $A^+$ heat-inactivated human plasma. Drug susceptibility was determined using the Malaria SYBR Green-I Fluorescence (MSF) assay (Johnson et al., 2007). Compounds were dissolved in DMSO at a concentration of 10 mM and were subsequently transferred to assay plates (Nunc MicroWell 384-well optical bottom) in duplicate using an ECHO 555 liquid handler. Final compound concentrations ranged between 0.03 and 24.90 μM (0.25% DMSO) to establish $IC_{50}$ values. Controls of 0.25% DMSO, no DMSO, and 110 μM amodiaquine were used to assess the quality of each plate. The D6 and C235 strains were sorbitol synchronized to the ring stage, added to the plate at an initial 0.3% parasitemia level and 2% hematocrit, and incubated for 72 h. The parasites were then lysed with 10 mM EDTA, 100 mM Tris-HCl (pH 7.5), 0.16% (w/v) saponin, and 1.6% (v/v) Triton X-100, mixed with SYBR Green-1 (1:10,000 dilution) and incubated in the dark for 24 h. Fluorescence was read using a Synergy H4 Hybrid Plate Reader (BioTek) (Exc: 485 nm, Em: 535 nm) with concentration response curves generated using the sigmoidal dose response variable slope curve fit on GraphPad Prism v5.0.

### 2.10. Antiplasmodial activity and genotoxicity study for chemical intermediates

The commercially available intermediate 4-(4-fluorophenyl)-1,2,3,6-tetrahydropyridine (**AM01**) and the synthesized intermediate 4-(4-nitro-2-trifluoromethylphenyl)aminopiperidine (**AM02**) were tested against *P. falciparum* FCR-3 multidrug resistant strain using the methodology followed to evaluate final compounds (14–26). Genotoxicity test SOS/*umu* was performed on **AM01** and **AM02** using the protocol followed to evaluate final compounds (**22**, **23**, **24**, and **25**). MetaSite software 3.0.4 (Molecular Discovery Ltd.) was used to predict human liver metabolism (site of metabolism) and potential metabolites using the P450 liver model that involves the three major liver isoforms (CYP3A4, CYP2C9, and CYP2D6). Although MetaSite does not have mouse CPY models, it is well known that these human isoforms have mouse homologs (Cui et al., 2012). To perform the predictions, MetaSite only used 3D structures of potential substrates as described by Cruciani et al. (2005). Structures were submitted to MetaSite as simplified molecular input line entry system notation (SMILES), the reactivity correction option and a minimal mass threshold of 50 Da for predicted metabolites were used. The site of metabolism is shown as soft spots graphic with a report as a histogram bar chart showing the probability of metabolism for any of the atoms.

### 2.11. Plasmepsin assay

PM2 (200 nM) was preincubated for 5 min, 37 °C in 0.1 M sodium formate, pH 4.4. Compounds dissolved in 100% DMSO were added to the enzyme for a final concentration of 5 μM (final DMSO concentration of 2%) and incubated with enzyme for 5 min. The preincubation time allows for complete conversion of the zymogen to active mature form of the enzyme. The reaction was initiated by the addition of 20 μM RS6 peptide (K-P-I-E-F-Nph-R-L). The substrate cleavage reaction was monitored by the decrease in the average absorbance from 284 to 324 nm on a Cary 50 Bio Varian spectrophotometer equipped with an 18-cell multitransport system. Reactions with inhibitor were compared to control reactions containing 2% DMSO only.

### 2.12. β-hematin inhibition assay

An *in vitro* assay developed by Sandlin et al. was used to test for β-hematin, abiological hemozoin, inhibition activity (Sandlin et al., 2011). Test compounds were screened between 0.44 and 110 μM with a final DMSO concentration of 0.25% in a clear 384-well flat bottom microtiter plate (Corning). Positive controls of 80 μM amodiaquine and negative controls of 0.25% DMSO were used to evaluate the validity of the assay. Following the addition of each compound, 20 μL of water and Nonidet P-40 detergent (30.5 μM final concentration) were added to each well to mediate crystal formation. A 25 mM hemin chloride stock was prepared in DMSO and was passed through a 0.22 μm PVDF membrane filter. From this stock solution, a 228-μM hematin suspension was prepared in 2 M acetate buffer (pH 4.8) and added to the plate for a final hematin concentration of 100 μM. After a 6 h shaking incubation at 37 °C, pyridine was added to the plate (5% v/v final concentration) and was shaken an additional hour. The absorbance of the pyridine-ferrochrome complex was measured at 405 nm using a Synergy H4 Hybrid Plate Reader (BioTek). Dose response curves were generated from the maximum absorbance values using a nonlinear regression of sigmoidal dose response variable slope curve fit on GraphPad Prism v5.0.

### 2.13. Target validation in P. falciparum

The compound's ability to affect the hemozoin formation pathway as a drug target was validated with the heme speciation assay (Combrinck et al., 2015). A D6 culture was sorbitol synchronized to the early ring stage and diluted to 5% parasitemia and 2% hematocrit. This culture was distributed in 2 mL aliquots to a 24-well flat bottom cell culture plate containing the test compound. A control sample of no drug was included alongside five varying concentrations, each in quadruplicate, based on the $IC_{50}$ values previously determined by the MSF assay. The plates were incubated at 37 °C, 5% $O_2$, 5% $CO_2$, and 90% $N_2$ for 32 h to allow for the parasite to reach the trophozoite stage. The mature parasites were then isolated from the erythrocytes through selective lysis with saponin (0.05% final concentration) and washed and resuspended in PBS. A 10 μL aliquot was removed from each sample for cell counting with the Countess II FL automated cell counter. The trophozoite pellet in PBS was fractionated into the three heme species: *P. falciparum* hemoglobin, free intracellular heme, and hemozoin as described by Combrinck et al. (2015). The maximum absorbance of the Fe (III) heme-pyridine complex that results from each of the fractionation steps was recorded at 405 nm in order to calculate the ratios of heme species in each sample.

### 2.14. Heme binding studies

Spectrophotometric titrations were conducted to further understand the interaction of each compound with the μ-oxo heme dimer *in vitro*. First, each compound was dissolved in 40% aqueous DMSO and 0.02 M HEPES (pH 7.4) and serial diluted into a clear 96-well microtiter plate in triplicate. A hemin solution in the same solvent system was added to the plate to a final concentration of 5 μM. The plate was incubated for 1 h in the dark prior to measuring the absorbance at 400 nm using a Synergy H4 Hybrid Plate Reader (BioTek). Titrations were conducted without the heme addition to account for any absorbance from the compound itself at 400 nm and these values were subtracted from the final results. Absorbance values were plotted using a nonlinear least squares fit with CurveFit v1.00 to determine the equilibrium association constant.

### 2.15. Three-dimensional pharmacophore model for new APD

The LigandScout software (Wolber and Langer, 2005) 4.09.2 (InteLigand GmbH Ltd.) was used to build and describe the pharmacophore models. Models were obtained using the ligand-based pharmacophore design that is implemented in the espresso module. For the APD model, the most active compounds were used as a training set (**22**, **23**, **24**, and **25**; FCR-3 $IC_{50} \leq 0.5$ μM), which included both possible enantiomers (*R* and *S* configurations) for each compound. For the classical arylamino alcohols (CAA), a consensus model was generated using the four molecules (quinine, mefloquine, lumefantrine, and halofantrine) and respective stereoisomers.

All molecules used in the pharmacophore study were drawn using ChemDraw Ultra software 7.0 (CambridgeSoft Ltd.) with stereoisomerism manually checked. Then, structures were submitted to LigandScout as SMILES. For each molecule, a three-dimensional (3D) multiconformational calculation was performed using the Icon conformer generation tool in LigandScout. The Best Setting option was used to generate the conformations (maximum number of conformations = 400, timeout = 600, RMS threshold = 0.8, energy window = 20, maximum pool size = 4000, and maximum fragment build time = 30). To generate models, the Merge Feature Pharmacophore option was used to take all the features into account and assemble them into one pharmacophore model (consensus model). The scoring function used to rank the models was Pharmacophore-Fit and Atom Overlap. The maximum number of pharmacophore models generated was ten. The model with the highest score was manually checked and considered as valid, since the model exhibited the molecules properly aligned. Pharmacophore representation including hydrophobic features (HPF), hydrogen bond donor features (HBDF), hydrogen bond acceptor features (HBAF), positive ionizable features (PIF), and aromatic ring features (ARF) were projected on molecules. For comparison of the final pharmacophore models (APD and CAA), a consensus model was constructed for APD. The *R* and *S* models were aligned using the alignment module in LigandScout. Both pharmacophores were merged and the overlapping features were interpolated. Finally, the new pharmacophore model for APD was aligned with the consensus pharmacophore model for CAA where only common features in both models were calculated and extracted.

## 3. Results and discussion

### 3.1. Separation and testing of the APD enantiomers

Chiral separation of compound **25** was made using ultra performance convergence chromatography with a Chiralpack IC column (Supplementary Data Fig. 1). There were no significant potency differences between the compound **25** enantiomers and racemic mixture against *P. falciparum* F32 Tanzania, chloroquine sensitive strain (F32 $IC_{50} \approx 0.50$ μM). The biological data for the two enantiomers of the compound **25** is shown in the Supplementary Data Table 1. Based on these results, we continued with synthesis and testing of the APD as racemates.

### 3.2. In vitro antiplasmodial activity (FCR-3 strain)

The activity of thirteen newly synthesized hydroxyl analogues (**14**–**26**) was determined against FCR-3 multidrug resistant strain (resistant to chloroquine, cycloguanil, and pyrimethamine) (Table 1). Chloroquine was used as a reference drug in all experiments for comparison (FCR-3 $IC_{50} = 0.13$ μM). Compounds **17**, **18**, **21**, **22**, **23**, **24**, **25**, and **26** all resulted in submicromolar activity (FCR-3 $IC_{50} < 1$ μM) with four of these below 0.5 μM (**22**, **23**, **24** and **25**).

Overall, incorporation of a single fluorine atom in the Ar (hydrophobic) region provided potency across the different benzo[*b*]thiophene, naphthalene, and benzene derivatives (Table 1, compounds **14**–**18** and **21**–**26**, $IC_{50} \leq 2.23$ μM). Compounds with a single fluorine atom in the Ar region (**23** and **26**) exhibited 35-fold and 9-fold increase in potency, respectively, compared to **19** and **20** (**23** vs **19** and **26** vs **20**), thereby confirming our previous observations of its requirement for antiplasmodial activity (Perez-Silanes et al., 2009; Mendoza et al., 2011). A good example of this observation is the comparison the $IC_{50}$ values of previous non-fluorinated analogues (* compounds) with new APD (see Supplementary Data Table 2, **14** vs ***7** and **15** vs ***8**). Exploration of the Ar region showed that 4-fluoro-1-naphthyl derivatives are 5-fold more active than 5-fluorobenzo[*b*]thiophenyl analogues (**18** vs **22**) and 1- to 3-fold more active than 4 fluoro-1-phenyl analogues (**23** vs **26** and **22** vs **25**) (Table 1). Interestingly, a particular study on ß-amino alcohols and their corresponding hydrophobic region must be highlighted due to its structural similarity with APD. Tacon et al. (2012) reported loss of antiplasmodial activity in derivatives compared with their corresponding totarol analogues. This loss of activity has involved the structural replacement of the totarol scaffold by simpler aromatic systems, common in APD, such as phenyl and naphthyl. As a result the compounds exhibited $IC_{50}$ values ranging between 5 and 100 μM (D10 strain, *P. falciparum*).

**Table 1**
*In vitro* antimalarial activity against multidrug-resistant strain (FCR-3) of *P. falciparum* and VERO cytotoxicity of compounds **14**–**26**.

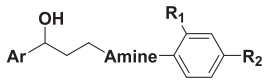


| Compound | Ar | Amine | $R_1$ | $R_2$ | FCR-3 $IC_{50}$ (μM)[a] | $CC_{50}$ (μM)[b] | SI[c] |
|---|---|---|---|---|---|---|---|
| 14 |  |  | $CF_3$ | $NO_2$ | 1.32 ± 0.20 | >200 | >150 |
| 15 |  |  | $NO_2$ | $CF_3$ | 2.23 ± 0.20 | >150 | >50 |
| 16 |  |  | H | $CF_3$ | 1.68 ± 0.60 | >250 | >100 |
| 17 |  |  | $CF_3$ | $NO_2$ | 0.75 ± 0.02 | 13.3 | 18 |
| 18 |  |  | $CF_3$ | $NO_2$ | 0.70 ± 0.10 | 6.3 | 9.00 |
| 19 |  |  | H | F | 14.03 ± 3.50 | 24.60 | 1.75 |
| 20 |  |  | H | F | 5.60 ± 2.30 | >350 | >50 |
| 21 |  |  | H | $CF_3$ | 0.93 ± 0.70 | >100 | >100 |
| 22 |  |  | $CF_3$ | $NO_2$ | 0.15 ± 0.01 | 5.5 | 37 |
| 23 |  |  | H | F | 0.40 ± 0.01 | 49.5 | 124 |
| 24 |  |  | $CF_3$ | $NO_2$ | 0.36 ± 0.14 | 88 | 244 |
| 25 |  |  | $CF_3$ | $NO_2$ | 0.48 ± 0.04 | 30.20 | 63 |
| 26 |  |  | H | F | 0.66 ± 0.01 | >100 | >150 |
| CQ[d] | | | | | 0.13 | >50 | |
| Doxorubicin | | | | | nt | 6.4 | nt |

[a] FCR-3 $IC_{50}$ values are the growth inhibition of 50% of *P. falciparum* parasites.
[b] $CC_{50}$ values are the inhibition of 50% of VERO cells survival.
[c] SI (selectivity index) = $CC_{50}$ (cytotoxicity)/$IC_{50}$ (FCR-3).
[d] CQ: chloroquine. nt: not tested.

Unfortunately, the authors did not explore the addition of a halogen atom in the hydrophobic portion.

It is noteworthy that electron-withdrawing groups at the para position on the phenyl ring such as -$CF_3$, -$NO_2$, and -F were well tolerated and resulted in highly active compounds (**21**, **22**, **23**, **24**, **25**, and **26**). By varying the position of the substituents from para to ortho (nitro group as $R_2$ and $R_1$ as trifluoromethyl group) the activity decreases (**14** vs **15**). This finding reinforced our preliminary observations that indicate the necessity of a hydrophobic group at the ortho position to improve activity (Mendoza et al., 2011). Additionally, when the trifluoromethyl group is substituted at the para position and the nitro group is removed, the activity remains almost unchanged (**14** $IC_{50}$ = 1.32 μM vs **16** $IC_{50}$ = 1.68 μM).

The central amine also influences the activity as seen with aminopiperidine analogues that are more active than piperazine analogues (**14** vs **18** and **21 vs 22** vs **23**). The same trend is observed when compound **22** is compared with an analogue previously published by our group where only piperazine was replaced (Mendoza et al., 2011). In relation to the exploration of arylamines, this finding is in agreement with the results reported by Molyneaux et al. (2005) that show unsubstituted amines (free NH) have significant antiplasmodial activity in resistant strains compared to their substituted analogues. One feasible explanation is that unsubstituted nitrogen (NH) may interact easily with possible targets, as there is a greater hydrogen bond capacity.

### 3.3. Cytotoxicity assay

The cytotoxicity of the thirteen newly synthesized hydroxyl analogues (**14**–**26**) was determined against VERO cells using the MTT-assay (Mosmann, 1983) (Table 1). The cytotoxic assays showed that analogues with aminopiperidine as the central amine are more cytotoxic than piperazine and tetrahydropyridine (**14** vs **18**, **24** vs **25**, and **22** vs **23** vs **26**, respectively). Additionally, Tacon et al. (2012) and our group have also reported low cytotoxicity in ß- and γ-amino alcohols with aryl-piperazinyl groups. In general, with the exception of compound **19**, all tetrahydropyridine and piperazine derivatives showed negligible cytotoxicity in VERO cells. In this context, an important criterion was the degree of selectivity of the APD that was expressed as selectivity index (SI) (Table 1), where a

greater SI value indicates increased selectivity for FCR-3 over VERO cells. The most active compounds (**22**, **23**, **24**, and **25**) showed moderate to high degree of selectivity index ($37 \leq SI \leq 244$).

### 3.4. In silico physicochemical properties (ADME profile)

A computational study was performed for the prediction of an ADME profile of all hydroxyl analogues (Table 2). Topological polar surface area (TPSA) is a good descriptor of drug absorbance in the intestines, Caco-2 monolayer penetration, and blood-brain barrier crossing (Ertl et al., 2000). TPSA was used to calculate the percentage of human intestinal absorption (%ABS) according to the equation: $\%ABS = 109-0.345 \times TPSA$, as shown by Zhao et al. (2002). In addition, Lipinski's rule of five (Lipinski et al., 1997) and the number of rotatable bonds (n-ROTB) (Veber et al., 2002) were also calculated in order to evaluate their druglikeness. From these parameters, all compounds exhibited a %ABS ranging between 80 and 100%. Only compounds **19** and **23** violated one Lipinski's parameter, **23** being at the limit (ALOGPs = 5). Therefore, the oral bioavailability of hydroxyl analogues could be considered interesting as agents for antimalarial therapy.

### 3.5. Genotoxicity assay

Studies to analyze the DNA-damaging effect or genotoxicity of the most active compounds were performed. The nitro substituent often causes safety concerns due to its well-documented mutagenic and carcinogenic potential (Purohit and Basu, 2000). Thus, the SOS/*umu* test was included as a preliminary genotoxicity screening assay because of the high degree of agreement between the SOS/*umu* test and the standardized Ames test (OECD guideline 471) (Reifferscheid and Heil, 1996). Compounds **22**, **23**, **24**, and **25** were not considered genotoxic since the induction factor (IF) was always lower than 2 at non-cytotoxic concentrations with or without S9 fraction (Supplementary Data Table 3). It should be noted, however, that in the first screening assay all the concentrations of **22** were cytotoxic (<80% survival) when tested in absence of metabolic activation and thus further testing at non-cytotoxic concentrations was needed to understand its genotoxic effects. A second screening test was performed at lower concentrations in order to have a larger range of non-cytotoxic concentrations (Supplementary Data Table 4). Again, none of the compounds showed an IF higher than two. Additionally, if a high degree of agreement between the SOS/*umu* test and Ames test was found (Reifferscheid and Heil, 1996), the SOS/*umu* test was used for screening purposes and selecting the best candidates. For regulatory purposes, negative results should be further evaluated with the standardized Ames test.

### 3.6. In vivo antimalarial activity

Along with the extensive SAR and toxicological studies, *in vivo* antimalarial activity in the *P. berghei* mouse model was evaluated following oral administration. The criteria to select compounds was based on FCR-3 $IC_{50} \leq 0.5$ μM, SI > 35, appropriate *in silico* bioavailability, and a negative genotoxicity test. Thus, parasitemia reduction and mean survival days (MSD) for chloroquine and promising APD compounds (**22**, **23**, **24**, and **25**) were evaluated at a unique oral dose (50 mg/kg × 4 days) (Table 3). Compound **22** displayed excellent parasitemia reduction (98± 1%), and complete cure with all treated mice surviving through the entire 21-day period with no signs of toxicity (MSD > 35). Compounds **23** and **25** showed parasitemia reduction of 73 ± 16% (MSD = 9) and 76 ± 30% (MSD = 5), respectively. Despite its antiplasmodial activity (FCR-3 $IC_{50} = 0.36$ μM), compound **24** was inferior in terms of *in vivo* parasitemia reduction (17 ± 8%; MSD = 8). Almost all previous studies on γ-to ß-amino alcohol have not carried out *in vivo* efficacy studies. Apart from our group (Perez-Silanes et al., 2009; Mendoza et al., 2011), only Bahamontes-Rosa et al. (2009) and Guy et al. (Lowes et al., 2012), have explored the *in vivo* efficacy of ß-amino alcohol with unsuccessful results (parasitemia reduction ≤ 60%). Thus, compounds **22**, **23**, and **25** appear as interesting compounds for future antimalarial programs, due to the agreement between *in vitro* and *in vivo* studies for these compounds.

### 3.7. In vitro antiplasmodial activity (D6 and C235 strains)

As previously mentioned, two important factors in developing APD as effective antimalarials are generating compounds with remarkable potency against both chloroquine sensitive and multidrug resistant strains of *P. falciparum*. In order to evaluate and validate the series quality (MMV, 2008), the $IC_{50}$ values for the best compounds were independently evaluated and validated in two laboratories utilizing two different strains of *P. falciparum*. Only three compounds with *in vivo* parasitemia reduction above 70% were tested against the D6 chloroquine sensitive (but naturally less

**Table 2**
*In silico* physicochemical properties of tested compounds (ADME profile).

| ID | %ABS | TPSA (Å$^2$) | *n*-ROTB | Molecular weight | ALOGPs 2.1 | *n*-OHNH Donors | *n*-ON acceptors | Lipinski's violations |
|---|---|---|---|---|---|---|---|---|
| rule | | | ≤10 | <500 | <5 | <5 | <10 | ≤1 |
| 14 | 84 | 72.5 | 7 | 483.49 | 4.47 | 1 | 6 | 0 |
| 15 | 84 | 72.5 | 7 | 483.50 | 4.49 | 1 | 6 | 0 |
| 16 | 100 | 26.7 | 6 | 438.49 | 4.83 | 1 | 3 | 0 |
| 17 | 84 | 72.5 | 7 | 497.51 | 4.81 | 1 | 6 | 0 |
| 18 | 81 | 81.3 | 8 | 497.51 | 4.31 | 2 | 6 | 0 |
| 19 | 100 | 23.5 | 5 | 361.46 | 5.27 | 1 | 2 | 1 |
| 20 | 100 | 23.5 | 6 | 379.74 | 4.41 | 1 | 2 | 0 |
| 21 | 100 | 26.7 | 6 | 432.46 | 4.77 | 1 | 3 | 0 |
| 22 | 81 | 81.3 | 8 | 491.47 | 4.39 | 2 | 6 | 0 |
| 23 | 100 | 23.5 | 5 | 379.45 | 5.00 | 1 | 2 | 1 |
| 24 | 84 | 72.5 | 7 | 427.44 | 3.75 | 1 | 6 | 0 |
| 25 | 81 | 81.3 | 8 | 441.47 | 3.47 | 2 | 6 | 0 |
| 26 | 100 | 23.5 | 5 | 329.39 | 4.12 | 1 | 2 | 0 |
| CQ | 99 | 28.2 | 8 | 319.90 | 5.28 | 1 | 3 | 1 |

%ABS: human intestinal absorption, calculated by: %ABS = 109-(0.345xTPSA); TPSA: topological polar surface area; n-ROTB: number of rotatable bonds; ALOGPs (LogP): logarithm of compound partition coefficient between n-octanol and water; n-OHNH: number of hydrogen bond donors; n-ON: number of hydrogen bond acceptors; CQ: chloroquine; molecular weight expressed as Dalton.

**Table 3**
*In vivo* antimalarial efficacy of selected compounds in *P. berghei*-infected mice.

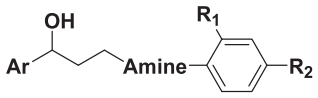


| Compound | Ar | Amine | $R_1$ | $R_2$ | % Suppression of parasitemia (MSD)[a] |
|---|---|---|---|---|---|
| 22 |  | 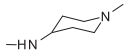 | $CF_3$ | $NO_2$ | 98 ± 1 (>35[b]) |
| 23 |  |  | H | F | 73 ± 16 (9) |
| 24 |  |  | $CF_3$ | $NO_2$ | 17 ± 8 (8) |
| 25 |  | 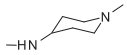 | $CF_3$ | $NO_2$ | 76 ± 30 (5) |
| CQ[c] | | | | | 87 ± 11 (16) |

[a] MSD = mean survival time (in days).
[b] Animals surviving beyond day 7 were monitored by examination of blood films every 7 days until day 35. At this time pooled blood was sub inoculated into clean mice and the absence of patent infection in these mice was verified until day 21 as evidence of curative activity.
[c] CQ: Chloroquine.

susceptible to mefloquine) and C235 multidrug resistant strain (resistant to mefloquine, chloroquine, and pyrimethamine) (Table 4).

Compounds **22** (D6 $IC_{50}$ = 0.11 μM, C235 $IC_{50}$ = 0.13 μM) and **23** (D6 $IC_{50}$ = 0.19 μM, C235 $IC_{50}$ = 0.28 μM) showed potent antimalarial activity in both strains. In contrast, compound **25** was less active against the multidrug resistant strain (D6 $IC_{50}$ = 0.49 μM, C235 $IC_{50}$ = 1.05 μM). Notably, like chloroquine (see Table 1), these APD compounds may act mechanistically different from mefloquine, a representative ß-amino alcohol, because of their high activity against the mefloquine resistant strain, and therefore, would not be affected by the same mechanism of mefloquine resistance. In addition, the resistance indices (RI, Supplementary Data Table 7) indicate that compounds **22** and **23** were slightly more active in the chloroquine sensitive strain. Compound **22** should be highlighted due to its *in vitro* submicromolar values, with equal potency against three different strains of *P. falciparum* (D6 $IC_{50}$ = 0.11 μM, C235 $IC_{50}$ = 0.13 μM, and FCR-3 $IC_{50}$ = 0.15 μM).

### 3.8. Antiplasmodial activity and genotoxicity study for chemical intermediates

When exploring new compounds, it is crucial to determine the lack of activity or genotoxicity of intermediates and potential metabolites early in the drug discovery process. In the case of APD, commercial or synthesized intermediates play a critical role for two reasons: (1) The Mannich reaction, a key step in our synthetic route, requires amines to obtain our ß-amino carbonyl intermediates (**1**–**13**) and thus, are an important fragment of the final compounds (**14**–**26**); (2) As a possible product of human or mouse P450-mediated oxidative metabolism of APD, these intermediates can be potential metabolites. To explore the activity profile, intermediates of the most active compounds (**22**, **23**, and **25**) were tested against *P. falciparum* FCR-3 chloroquine resistant strain

**Table 4**
*In vitro* antimalarial activity against chloroquine sensitive strain (D6) and multidrug-resistant strain (C235) of *P. falciparum*.

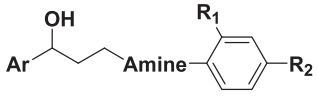


| Compound | Ar | Amine | $R_1$ | $R_2$ | Antimalarial activity $IC_{50}$ (μM) | | β-hematin inhibition activity $IC_{50}$ (μM) |
|---|---|---|---|---|---|---|---|
| | | | | | D6 | C235 | |
| 22 |  | 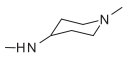 | $CF_3$ | $NO_2$ | 0.11 ± 0.01 | 0.13 ± 0.01 | 80.7 ± 1.7 |
| 23 |  |  | H | F | 0.19 ± 0.04 | 0.28 ± 0.05 | Not active |
| 25 |  | 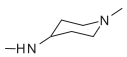 | $CF_3$ | $NO_2$ | 0.49 ± 0.07 | 1.05 ± 0.02 | Not active |
| CQ | | | | | 0.014 ± 0.001 | 0.048 ± 0.004 | 48.7 ± 2.7 |

**Table 5**
*In vitro* antimalarial activity against *P. falciparum* multidrug-resistant strain (FCR-3) of selected intermediates (potential metabolites).

| Intermediate | Chemical structure | $IC_{50}$ (μM) |
|---|---|---|
| | | FCR-3 |
| AM01 | 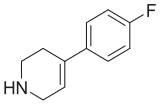 | 8.2 ± 2.0 |
| AM02 | 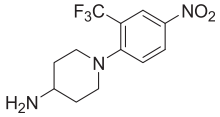 | 4.3 ± 0.9 |

(Table 5). Intermediates **AM01** and **AM02** ($IC_{50}$ = 8.2 μM and $IC_{50}$ = 4.3 μM, respectively) showed low antiplasmodial activity compared to their final products. To explore the probability of obtaining the corresponding intermediates as potential metabolites, an *in silico* approach using MetaSite software was performed. This approach allowed for a simple, fast, and inexpensive method of identifying the most probable site of metabolism (SoM) of the most active compounds and therefore, predicts P450-derived metabolites. As shown in Fig. 2, MetaSite predicted the P450 2C9-, P450 3A4-, and P450 2D6-catalyzed *N*-dealkylation of **22**, **23**, and **25** as the most probable biotransformation pathway. Our predictions indicated that *N*-dealkylation would occur principally on the side chain α-carbon hydrogen(s) next to the amino aliphatic nitrogen for **22** and **25**, and next to the tertiary amine for **23**. In fact, our results were reinforced by experimental and theoretical data found where the metabolism of 4-aminopiperidine drugs were well studied (Sun and Scott, 2011). Genotoxicity profiles of intermediates (potential metabolites) were performed using the SOS/*umu* test as a screening test (Supplementary Data Table 5). Intermediates **AM01** and **AM02** were not considered genotoxic as the IF was always lower than 2 at non-cytotoxic concentrations with or without S9 fraction. Thus, it can be deduced that *in vitro* and *in vivo* antimalarial activity of compounds **22**, **23**, and **25** is associated with the entire molecule and not only to the amine scaffold intermediate. Additionally, the viability to find an intermediate as a product of CYP biotransformation exists. Genotoxicity assay of potential metabolites reinforce no genotoxic results observed with metabolic activation on APD. It should be noted that Metasite and SOS/*umu* approaches were used for screening purposes and initial studies. More in depth studies must be performed using standard assays such as the Ames test and human or rat liver microsomal stability.

### 3.9. Target exploration of plasmepsin II

Based on previous *in silico* studies performed by our group (Mendoza et al., 2011), PM2 enzyme was proposed as a putative target for APD. PM2, which is involved in the initial steps of hemoglobin degradation, plays a critical role in the intraerythrocytic cycle of the parasite. Consequently, in recent years PM2 has sparked interest in the antimalarial community (Marvin and Daniel, 2012). Docking studies showed a possible mode of union associated with good affinity values (Gibbs free energy). To confirm our predictions, eight compounds synthesized in this manuscript with antiplasmodial FCR-3 $IC_{50}$ values ranging between 0.15 and 1.7 μM were tested against PM2. Compounds **14**, **16**, **17**, **18**, **22**, **23**, **24**, and **25** (tested at 5 μM) showed no significant inhibition of PM2 compared to the control (Supplementary Data Table 6). Thus, PM2 was discarded as a target for APD. Interestingly, our findings were better understood when we compared our results with other hybrid studies (computational and experimental approaches). Friedman and Caflisch (2009) performed high-throughput docking simulations using consensus-scoring methods to screen a database of 40,000 molecules resulting in 11 arylamino alcohols, halofantrine and 10 structurally related to halofantrine and lumefantrine, that were plasmepsin inhibitors (PM1, PM2, and PM3). Important facts when analyzing and comparing our results include the following: (1) Halofantrine shares the γ-amino alcohol moiety with APD (Fig. 1); (2) According to the proposed docking experiments, halofantrine may share the same theoretical binding mode as APD (Friedman and Caflisch, 2009; Mendoza et al., 2011). This binding mode includes one hydrogen bond between the oxygen of the hydroxyl group and Asp214 and electrostatic interactions between the nitrogen of the tertiary or secondary amine located near the charged Asp34; (3) The unique major structural differences between APD and halofantrine (or its derivatives) are the aliphatic chains of the four carbon length bond to the tertiary amine that are

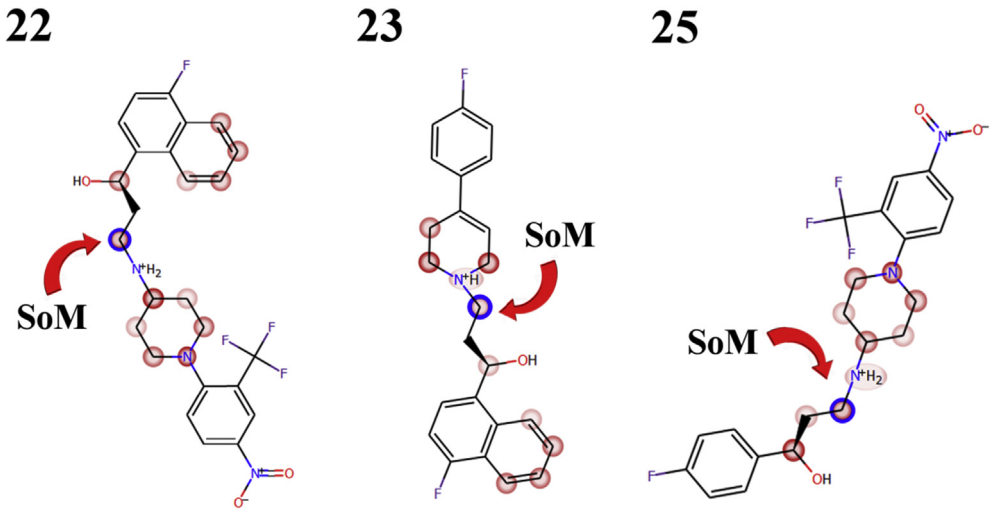


**Fig. 2.** Plots of MetaSite predictions for sites of metabolism (SoM) for compounds **22**, **23**, and **25**. Predictions were performed using the P450 liver model that involves three major liver isoforms (CYP3A4, CYP2C9, and CYP2D6). Red arrows indicate the most probable site of metabolism. Soft spots intensity represents the potential metabolic sites probability.(For interpretation of the references to colour in this figure legend, the reader is referred to the web version of this article.)

not present in APD, and (4) The $IC_{50}$ values reported by Friedman and Caflish (2009) for the 11 arylamino alcohols are considered medium to low (2 μM ≤ $IC_{50}$ ≤ 100 μM), when compared with other well-known plasmepsin inhibitors ($IC_{50}$ ≤ 0.01 μM) (Marvin and Daniel, 2012). Based on these results, we reinforce the hypothesis that the primary mechanism of action of arylamino alcohols such as APD, halofantrine, lumefantrine, and mefloquine is not through plasmepsin inhibition. Therefore, in depth studies related to alternative mechanisms of action must be performed with APD. Additionally, while computational methodologies are valuable tools, even well validated methodologies can produce false positives. For example, Degliesposti et al. (2009) designed and developed a rigorous *in silico* pipeline to observe PM2 inhibition, yet still obtained four false positives of thirty compounds tested. Further, future APD could be useful for the antimalarial drug discovery community as decoys or negative controls for *in silico* high-throughput screening campaigns to identify PM2 inhibitors (similar physicochemical properties, but structurally dissimilar to APD) (Huang et al., 2006).

### 3.10. Target exploration of the hemozoin formation pathway

The compounds with both *in vivo* and *in vitro* antiplasmodial activity against *P. berghei and P. falciparum*, respectively, were further tested against the hemozoin formation drug target pathway to understand the mechanism of action. The *in vitro* β-hematin inhibition assay established by Sandlin et al. (2011) was utilized for these three compounds (**22**, **23**, and **25**). Only compound **22** was found to inhibit β-hematin formation with an $IC_{50}$ of 80.7 ± 1.7 μM (Table 4). The affinity of compound **22** for the μ-oxo dimer form of heme was shown through a binding curve with **22**. When compared to positive and negative control compound binding curves (chloroquine and pyrimethamine, respectively), compound **22** exhibited affinity resembling that of chloroquine (Supplementary Data Fig. 2), a known hemozoin inhibitor. To further explore the mechanism of action of compound **22**, target validation of the hemozoin formation pathway was conducted in a culture of parasites. Examination of the three species of parasitic heme (host ingested hemoglobin, intracellular free heme, and hemozoin) revealed that the primary mode of action for compound **22** is not through hemozoin formation inhibition. Despite a decline in parasite viability with increasing concentrations of compound, the levels of free heme and hemozoin remained constant. Therefore, the hemozoin formation pathway is not the predominant mode of death when a culture of parasite is subjected to compound **22**. While our *in vitro* assay used has previously resulted in the highest hit rate and lowest false positive rates amongst other β-hematin inhibition assays (Sandlin et al., 2014), there are still limits. This plate assay closely resembles the biological environment of the site of hemozoin formation, but target validation is vital to ensure that the *in vitro* results translate to a parasite culture. One hypothesis is that compound **22** inhibits hemozoin formation; however, secondarily to a more potent mechanism of action, causing the levels of heme species to remain unchanged.

### 3.11. Three-dimensional pharmacophore model for new APD

A pharmacophore for arylamino alcohols is defined as the general structural requirements necessary for its antiplasmodial activity (Fig. 1). This definition led us to ask: Are APD like any of the historical arylamino alcohols? Do they share the same pharmacophore? Based on *in vitro*, *in vivo*, and target exploration results, we investigated the structural similarities and differences between APD and CAA (quinine, mefloquine, lumefantrine, and halofantrine) using 3D pharmacophore models. First, we constructed and analyzed an *in silico* 3D pharmacophore model for the new APD. Second, the resulting 3D pharmacophore model for APD was compared with the *in silico* 3D pharmacophore model of CAA in order to identify common features between APD and CAA. Although two-dimensional (2D) pharmacophore models could be inferred from Fig. 1, these models lack 3D arrangements (3D conditional patterns), which are important at the moment to study potential modes of union between ligands and macromolecules.

Two 3D pharmacophore models (*R* and *S* configuration) were generated for APD (Fig. 3a), resulting in similar features, but a different 3D arrangement of the naphthyl group. Then, both models were aligned and the pharmacophoric features were merged into a unique model, creating a consensus pharmacophore (Fig. 3b). The final model consisted of four HPF, one PIF, two ARF, seven HBAF, and one HBDF. Due to the absence of the trifluoromethyl group in compound **23**, these substituent features were presented as optional (dot lines) in the model. A detailed summary of the pharmacophoric features for each compound is presented in Supplementary Data Fig. 3. A consensus pharmacophore model for CAA was also generated (Fig. 3b), consisting of four HPF, one PIF, two ARF, one HBDF, and one HBAF. Two HPF were shown as optional since mefloquine and quinine do not share identical features with halofantrine and lumefantrine. Additionally, one ARF was shown as optional due to lumefantrine not sharing this feature with quinine, halofantrine, and mefloquine.

The consensus pharmacophore models for APD and CAA were aligned and the common features were extracted (Fig. 3b), including two HPF, one PIF, one ARF, one HBDF, and one HBAF. All six features were mandatory in APD and CAA (no optional features). Our findings are in agreement with the general description that Bhattacharjee et al. (1996) reported for the arylamino alcohol chemotype (Fig. 1). Specifically for APD, these common features are observed in the hydrophobic (naphthyl and phenyl system) and the amine region of the scaffold; however, APD exhibited nine differences in comparison with CAA (two HPF, one ARF, and six HBAF). These pharmacophore differences may explain the lack of inhibition with the PM2 enzyme and hemozoin pathway. Thus, only a 40% (6/15) of similarity between APD and CAA was observed at the pharmacophore level.

## 4. Conclusions

This manuscript has shown the synthesis, racemic separation, *in silico* drug-likeness studies, *in vitro* evaluation against chloroquine sensitive (F32 and D6) and multidrug resistant (FCR-3 and C235) strains of *P. falciparum*, cytotoxicity (VERO), *in silico* metabolism studies, genotoxicity, *in vivo* efficacy in *P. berghei* mouse model, target exploration, and pharmacophore modeling of new APD.

This work led to the identification of four promising compounds (**22**, **23**, **24**, and **25**) that exhibit values of antiplasmodial activity below 0.5 μM (FCR-3), appropriate drug-likeness profile, adequate selectivity index (37 ≤ SI ≤ 244), and absence of genotoxicity. *In vivo* efficacy in *P. berghei* mouse model showed APD **22**, **23**, and **25** as promising candidates. Notably, compound **22** displayed excellent parasitemia reduction (98 ± 1%) and complete cure with all treated mice surviving through the entire 21-day period with no signs of toxicity. Additionally, compounds **22** and **23** showed potent antimalarial activity in chloroquine sensitive and multidrug resistant strains (D6 $IC_{50}$ ≤ 0.19 μM, C235 $IC_{50}$ ≤ 0.28 μM). Target exploration was performed in order to establish a possible mechanism of action; however, both the PM2 enzyme and the hemozoin inhibition pathway were ruled out as primary targets for APD. Comparison of 3D pharmacophore models indicated only a 40% similarity between APD and CAA. This similarity consisted of two HPF, one PIF, one ARF, one HBDF, and one HBAF.

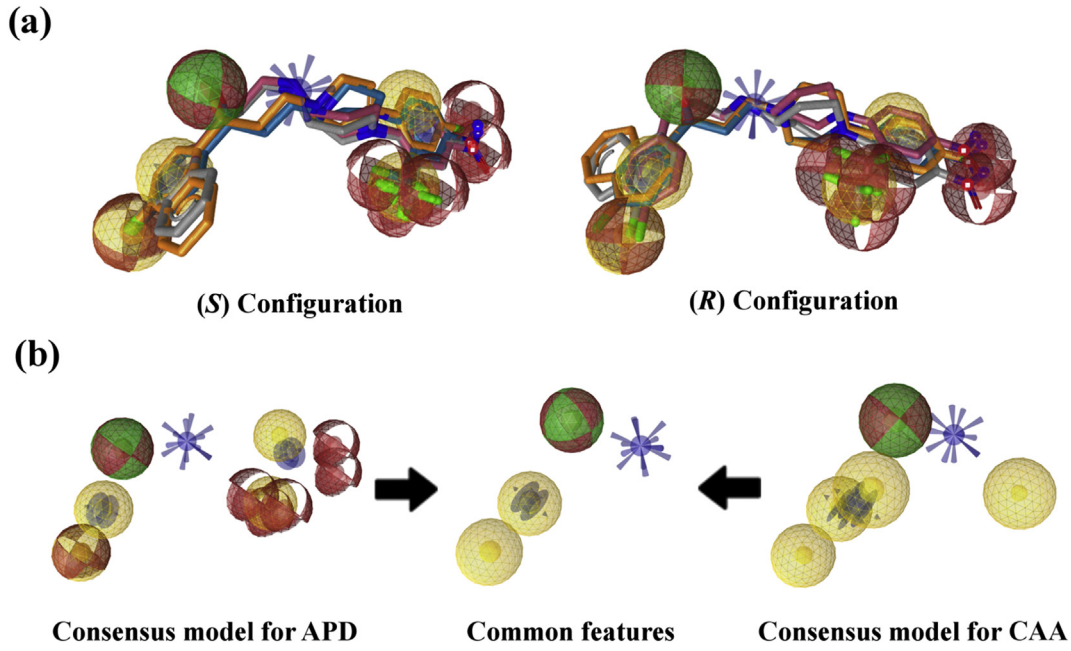


**Fig. 3.** Three-dimensional pharmacophore model for new APD: (a) 3D pharmacophore models for APD; (b) Consensus pharmacophore models for APD and CAA, and its common features.

This series of new APD showed not only promising *in vitro* and *in vivo* efficacy values, but also exhibited agreement between *in vitro* and *in vivo* studies. This last point is important due to the large number of potent antimalarial compounds reported in the literature that are only efficacious at *in vitro* and will no longer proceed along the drug discovery pipeline. APD are promising compounds as new antimalarial therapeutics not only for their particular unexplored chemotype, but also for their unknown mechanism of action, which we found to differ from chloroquine or classical amino alcohols. Further optimization of the scaffold must be done through complementary SAR, mechanistic, and pharmacology studies.

## Author's contributions

The manuscript was written through contributions of all authors. All authors have given approval to the final version of the manuscript. The authors declared that there is no conflict of interest.

## Acknowledgments

This work was supported by PIUNA Project-University of Navarra and Foundation CAN (grant number: 70391). The authors are grateful to Universidad de Antioquia for its Sustainability Strategic Plan and the Institute of Tropical Health (ISTUN) of University of Navarra for the financial support and help. Miguel Quiliano is grateful to "Programa Nacional de Innovación para la competitividad y productividad" (Innóvate-Perú) for his PhD scholarship (grant 065-FINCYT-BDE-2014). Adela Mendoza acknowledges ADA (University of Navarra) for a PhD scholarship. The authors thank MF Richards for critical reading of this manuscript.

## Appendix A. Supplementary data

Supplementary data related to this article can be found at http://dx.doi.org/10.1016/j.ijpddr.2016.09.004.

## References

Andrews, K.T., Fisher, G., Skinner-Adams, T.S., 2014. Drug repurposing and human parasitic protozoan diseases. Int. J. Parasitol. Drugs Drug Resist 4, 95–111.
Ashley, E.A., Dhorda, M., Fairhurst, R.M., Amaratunga, C., Lim, P., Suon, S., Sreng, S., Anderson, J.M., Mao, S., Sam, B., Sopha, C., Chuor, C.M., Nguon, C., Sovannaroth, S., Pukrittayakamee, S., Jittamala, P., Chotivanich, K., Chutasmit, K., Suchatsoonthorn, C., Runcharoen, R., Hien, T.T., Thuy-Nhien, N.T., Thanh, N.V., Phu, N.H., Htut, Y., Han, K.-T., Aye, K.H., Mokuolu, O.A., Olaosebikan, R.R., Folaranmi, O.O., Mayxay, M., Khanthavong, M., Hongvanthong, B., Newton, P.N., Onyamboko, M.A., Fanello, C.I., Tshefu, A.K., Mishra, N., Valecha, N., Phyo, A.P., Nosten, F., Yi, P., Tripura, R., Borrmann, S., Bashraheil, M., Peshu, J., Faiz, M.A., Ghose, A., Hossain, M.A., Samad, R., Rahman, M.R., Hasan, M.M., Islam, A., Miotto, O., Amato, R., MacInnis, B., Stalker, J., Kwiatkowski, D.P., Bozdech, Z., Jeeyapant, A., Cheah, P.Y., Sakulthaew, T., Chalk, J., Intharabut, B., Silamut, K., Lee, S.J., Vihokhern, B., Kunasol, C., Imwong, M., Tarning, J., Taylor, W.J., Yeung, S., Woodrow, C.J., Flegg, J.A., Das, D., Smith, J., Venkatesan, M., Plowe, C.V., Stepniewska, K., Guerin, P.J., Dondorp, A.M., Day, N.P., White, N.J., 2014. Spread of artemisinin resistance in Plasmodium falciparum malaria. N. Engl. J. Med. 371, 411–423.
Bahamontes-Rosa, N., Bucher, K., Held, J., Robin, A., Hoffmann, W.H., Flitsch, S.L., Kremsner, P.G., Kun, J.F.J., 2009. In vivo anti-malarial effect of the ß-amino alcohol 1t on Plasmodium berghei. Parasitol. Res. 104, 1459–1464.
Barnett, D.S., Guy, R.K., 2014. Antimalarials in development in 2014. Chem. Rev. 114, 11221–11241.
Bhattacharjee, A.K., Karle, J.M., 1996. Molecular electronic properties of a series of 4-Quinolinecarbinolamines define antimalarial activity profile. J. Med. Chem. 39, 4622–4629.
Biamonte, M.A., 2014. Realistically, how far are we from a universal malaria drug? Future Med. Chem. 6, 123–126.
Biamonte, M.A., Wanner, J., Le Roch, K.G., 2013. Recent advances in malaria drug discovery. Bioorg. Med. Chem. Lett. 23, 2829–2843.
Bouquet, J., Rivaud, M., Chevalley, S., Deharo, E., Jullian, V., Valentin, A., 2012. Biological activities of nitidine, a potential anti-malarial lead compound. Malar. J. 11, 1–8.
Clarkson, C., Musonda, C.C., Chibale, K., Campbell, W.E., Smith, P., 2003. Synthesis of totarol amino alcohol derivatives and their antiplasmodial activity and cytotoxicity. Bioorg. Med. Chem. 11, 4417–4422.
Combrinck, J., Fong, K., Gibhard, L., Smith, P., Wright, D., Egan, T., 2015. Optimization of a multi-well colorimetric assay to determine haem species in Plasmodium falciparum in the presence of anti-malarials. Malar. J. 14, 253.
Cruciani, G., Carosati, E., De Boeck, B., Ethirajulu, K., Mackie, C., Howe, T., Vianello, R., 2005. MetaSite: understanding metabolism in human cytochromes from the perspective of the chemist. J. Med. Chem. 48, 6970–6979.
Cui, J.Y., Renaud, H.J., Klaassen, C.D., 2012. Ontogeny of novel cytochrome P450 gene isoforms during postnatal liver maturation in mice. Drug Metab. Dispos. 40, 1226–1237.
D'hooghe, M., Dekeukeleire, S., Mollet, K., Lategan, C., Smith, P.J., Chibale, K., De

Kimpe, N., 2009. Synthesis of novel 2-Alkoxy-3-amino-3-arylpropan-1-ols and 5-Alkoxy-4-aryl-1,3-oxazinanes with antimalarial activity. J. Med. Chem. 52, 4058–4062.
D'hooghe, M., Vandekerckhove, S., Mollet, K., Vervisch, K., Dekeukeleire, S., Lehoucq, L., Lategan, C., Smith, P.J., Chibale, K., De Kimpe, N., 2011. Synthesis of 2-amino-3-arylpropan-1-ols and 1-(2,3-diaminopropyl)-1,2,3-triazoles and evaluation of their antimalarial activity. Beilstein J. Org. Chem. 7, 1745–1752.
Degliesposti, G., Kasam, V., Da Costa, A., Kang, H.-K., Kim, N., Kim, D.-W., Breton, V., Kim, D., Rastelli, G., 2009. Design and discovery of plasmepsin II inhibitors using an automated workflow on large-scale grids. ChemMedChem 4, 1164–1173.
Delves, M., Plouffe, D., Scheurer, C., Meister, S., Wittlin, S., Winzeler, E.A., Sinden, R.E., Leroy, D., 2012. The activities of current antimalarial drugs on the life cycle stages of Plasmodium: a comparative study with human and rodent parasites. PLoS Med. 9, e1001169.
Desjardins, R.E., Canfield, C.J., Haynes, J.D., Chulay, J.D., 1979. Quantitative assessment of antimalarial activity in vitro by a semiautomated microdilution technique. Antimicrob. Agents Chemother. 16, 710–718.
Ertl, P., Rohde, B., Selzer, P., 2000. Fast calculation of molecular polar surface area as a sum of fragment-based contributions and its application to the prediction of drug transport properties. J. Med. Chem. 43, 3714–3717.
Friedman, R., Caflisch, A., 2009. Discovery of plasmepsin inhibitors by fragment-based docking and consensus scoring. ChemMedChem 4, 1317–1326.
Hans, R.H., Gut, J., Rosenthal, P.J., Chibale, K., 2010. Comparison of the antiplasmodial and falcipain-2 inhibitory activity of beta-amino alcohol thiolactone-chalcone and isatin-chalcone hybrids. Bioorg. Med. Chem. Lett. 20, 2234–2237.
Huang, N., Shoichet, B.K., Irwin, J.J., 2006. Benchmarking sets for molecular docking. J. Med. Chem. 49, 6789–6801.
Huber, W., Koella, J.C., 1993. A comparison of three methods of estimating EC50 in studies of drug resistance of malaria parasites. Acta Trop. 55, 257–261.
Johnson, J.D., Dennull, R.A., Gerena, L., Lopez-Sanchez, M., Roncal, N.E., Waters, N.C., 2007. Assessment and continued validation of the malaria SYBR green I-Based fluorescence assay for use in malaria drug screening. Antimicrob. Agents Chemother. 51, 1926–1933.
Kobarfard, F., Yardley, V., Little, S., Daryaee, F., Chibale, K., 2012. Synthesis of aminoquinoline-based aminoalcohols and oxazolidinones and their antiplasmodial activity. Chem. Biol. Drug Des. 79, 326–331.
Lipinski, C.A., Lombardo, F., Dominy, B.W., Feeney, P.J., 1997. Experimental and computational approaches to estimate solubility and permeability in drug discovery and development settings. Adv. Drug Deliv. Rev. 23, 3–25.
Lowes, D., Pradhan, A., Iyer, L.V., Parman, T., Gow, J., Zhu, F., Furimsky, A., Lemoff, A., Guiguemde, W.A., Sigal, M., Clark, J.A., Wilson, E., Tang, L., Connelly, M.C., DeRisi, J.L., Kyle, D.E., Mirsalis, J., Guy, R.K., 2012. Lead optimization of antimalarial propafenone analogues. J. Med. Chem. 55, 6087–6093.
Lowes, D.J., Guiguemde, W.A., Connelly, M.C., Zhu, F., Sigal, M.S., Clark, J.A., Lemoff, A.S., Derisi, J.L., Wilson, E.B., Guy, R.K., 2011. Optimization of propafenone analogues as antimalarial leads. J. Med. Chem. 54, 7477–7485.
Marvin, J.M., Daniel, E.G., 2012. Recent advances in plasmepsin medicinal Chemistry and implications for future antimalarial drug discovery efforts. Curr. Top. Med. Chem. 12, 445–455.
Mendoza, A., Perez-Silanes, S., Quiliano, M., Pabon, A., Galiano, S., Gonzalez, G., Garavito, G., Zimic, M., Vaisberg, A., Aldana, I., Monge, A., Deharo, E., 2011. Aryl piperazine and pyrrolidine as antimalarial agents. Synthesis and investigation of structure-activity relationships. Exp. Parasitol. 128, 97–103.
Milner, E., McCalmont, W., Bhonsle, J., Caridha, D., Cobar, J., Gardner, S., Gerena, L., Goodine, D., Lanteri, C., Melendez, V., Roncal, N., Sousa, J., Wipf, P., Dow, G.S., 2010. Anti-malarial activity of a non-piperidine library of next-generation quinoline methanols. Malar. J. 9, 51–51.
MMV, 2008. MMV Compound Progression Criteria.
Molyneaux, C.-A., Krugliak, M., Ginsburg, H., Chibale, K., 2005. Arylpiperazines displaying preferential potency against chloroquine-resistant strains of the malaria parasite Plasmodium falciparum. Biochem. Pharmacol. 71, 61–68.
Mosmann, T., 1983. Rapid colorimetric assay for cellular growth and survival: application to proliferation and cytotoxicity assays. J. Immunol. Methods 65, 55–63.
Oda, Y., Nakamura, S.-i., Oki, I., Kato, T., Shinagawa, H., 1985. Evaluation of the new system (umu-test) for the detection of environmental mutagens and carcinogens. Mutat. Res. Genet. Toxicol. Environ. Mutagen 147, 219–229.
Perez-Silanes, S., Berrade, L., Garcia-Sanchez, R., Mendoza, A., Galiano, S., Perez-Solorzano, B., Nogal-Ruiz, J., Martinez-Fernandez, A., Aldana, I., Monge, A., 2009. New 1-Aryl-3-Substituted propanol derivatives as antimalarial agents. Molecules 14, 4120.
Peters, W., 1970. Chemotherapy and Drug Resistance in Malaria. Academic Press, London.
Purohit, V., Basu, A.K., 2000. Mutagenicity of nitroaromatic compounds. Chem. Res. Toxicol. 13, 673–692.
Quiliano, M., Aldana, I., 2013. Quinoxaline and arylaminoalcohol derivatives as antiplasmodial and leishmanicidal agents: a review of our first ten years in the field. Rev. Virtual Quim. 5, 1120–1123.
Reifferscheid, G., Heil, J., Oda, Y., Zahn, R.K., 1991. A microplate version of the SOS/umu-test for rapid detection of genotoxins and genotoxic potentials of environmental samples. Mutat. Res. Genet. Toxicol. Environ. Mutagen 253, 215–222.
Reifferscheid, G., Heil, J.r, 1996. Validation of the SOS/umu test using test results of 486 chemicals and comparison with the Ames test and carcinogenicity data. Mutat. Res. Genet. Toxicol. Environ. Mutagen 369, 129–145.
Robin, A., Brown, F., Bahamontes-Rosa, N., Wu, B., Beitz, E., Kun, J.F.J., Flitsch, S.L., 2007. Microwave-assisted ring opening of epoxides: a general route to the synthesis of 1-Aminopropan-2-ols with anti malaria parasite activities. J. Med. Chem. 50, 4243–4249.
Sandlin, R.D., Carter, M.D., Lee, P.J., Auschwitz, J.M., Leed, S.E., Johnson, J.D., Wright, D.W., 2011. Use of the NP-40 detergent-mediated assay in discovery of Inhibitors of beta-hematin crystallization. Antimicrob. Agents Chemother. 55, 3363–3369.
Sandlin, R.D., Fong, K.Y., Wicht, K.J., Carrell, H.M., Egan, T.J., Wright, D.W., 2014. Identification of β-hematin inhibitors in a high-throughput screening effort reveals scaffolds with in vitro antimalarial activity. Int. J. Parasitol. Drugs Drug Resist. 4, 316–325.
Sun, H., Scott, D.O., 2011. Metabolism of 4-Aminopiperidine drugs by cytochrome P450s: molecular and quantum mechanical insights into drug design. ACS Med. Chem. Lett. 2, 638–643.
Tacon, C., Guantai, E.M., Smith, P.J., Chibale, K., 2012. Synthesis, biological evaluation and mechanistic studies of totarol amino alcohol derivatives as potential antimalarial agents. Bioorg. Med. Chem. 20, 893–902.
Tetko, I., Gasteiger, J., Todeschini, R., Mauri, A., Livingstone, D., Ertl, P., Palyulin, V., Radchenko, E., Zefirov, N., Makarenko, A., Tanchuk, V., Prokopenko, V., 2005. Virtual computational Chemistry laboratory - design and description. J. Comput. Aided Mol. Des. 19, 453–463.
Trager, W., Jensen, J.B., 1976. Human malaria parasites in continuous culture. Science 193, 673–675.
Tun, K.M., Imwong, M., Lwin, K.M., Win, A.A., Hlaing, T.M., Hlaing, T., Lin, K., Kyaw, M.P., Plewes, K., Faiz, M.A., Dhorda, M., Cheah, P.Y., Pukrittayakamee, S., Ashley, E.A., Anderson, T.J.C., Nair, S., McDew-White, M., Flegg, J.A., Grist, E.P.M., Guerin, P., Maude, R.J., Smithuis, F., Dondorp, A.M., Day, N.P.J., Nosten, F.ß., White, N.J., Woodrow, C.J., 2015. Spread of artemisinin-resistant Plasmodium falciparum in Myanmar: a cross-sectional survey of the K13 molecular marker. Lancet Infect. Dis. 15, 415–421.
Veber, D.F., Johnson, S.R., Cheng, H.-Y., Smith, B.R., Ward, K.W., Kopple, K.D., 2002. Molecular properties that influence the oral bioavailability of drug candidates. J. Med. Chem. 45, 2615–2623.
Weisman, J.L., Liou, A.P., Shelat, A.A., Cohen, F.E., Kiplin Guy, R., DeRisi, J.L., 2006. Searching for new antimalarial therapeutics amongst known drugs. Chem. Biol. Drug Des. 67, 409–416.
Wells, T.N.C., van Huijsduijnen, R.H., Van Voorhis, W.C., 2015. Malaria medicines: a glass half full? Nat. Rev. Drug Discov. 14, 424–442.
WHO, 2015. World Malaria Report 2015. World Health Organization, Geneva, Switzerland.
Wolber, G., Langer, T., 2005. LigandScout: 3-D pharmacophores derived from protein-bound ligands and their use as virtual screening filters. J. Chem. Inf. Model 45, 160–169.
Zhao, Y., Abraham, M., Le, J., Hersey, A., Luscombe, C., Beck, G., Sherborne, B., Cooper, I., 2002. Rate-limited steps of human oral absorption and QSAR studies. Pharm. Res. 19, 1446–1457.